EFFECT OF SOIL STRENGTH AND VEGETATION ON MARSH EDGE EROSION FOR LOUISIANA COASTAL PROTECTION AND RESTORATION

Final Report

Undergraduate Research Opportunities Program (UROP)

Louisiana Sea Grant

Project Technical Area:	Living Resources: Recovery and Utilization	
Project Duration	Start Date: 03/01/2017	End Date: 12/31/2017

Student Name:	Brendan Copley
Major:	Civil Engineering
Department:	Civil and Environmental Engineering
Major:	Civil Engineering
E-Mail Address:	bcople1@lsu.edu

Faculty Advisor's Name:	PI: Navid H. Jafari	
Department:	Civil and Environmental Engineering	
Affiliation:	Louisiana State University	
Phone Number:	(225) 578-8475	
E-Mail Address:	njafari@lsu.edu	

EXECUTIVE SUMMARY

Wetland loss along Louisiana's coast presents an urgent risk to natural habitats, coastal communities, and both local and national industries. A key natural cause of coastal erosion is continuous wave action along marsh edges. Moreover, coastal wetlands are frequently subject to surge and stronger wave forces brought about by tropical storms and hurricanes. The scarcity of synchronized field data of waves, currents, soil, and vegetation near a marsh edge limits the existing capability for predicting marsh edge erosion rate as a function of wave power, and soil and vegetation properties. The proposed research aims to enhance the fidelity of marsh edge erosion predictions for improved coastal restoration and management through data collection and the implementation of a continuously-monitored site in Terrebonne Bay. In-situ cone penetration tests will help determine the relationship between soil shear strength (across varying habitat types) on erosional resistance. Spatial and temporal trends in soil strength are anticipated to clarify why certain locations erode faster than other areas. The proposed methodology for marsh edge monitoring incorporates photogrammetry through the placement of cameras at frontal and lateral views. This novel approach will be used to identify the frequency and evolution of marsh retreat, and will assist long-term efforts at developing a mechanistic erosion model. The success of future marsh creation projects implemented by state agencies will be fortified by a more robust understanding of the geotechnical parameters affecting marsh edge erosion and the physical processes that lead to coastal land loss.

1. INTRODUCTION

Wetland loss on the hurricane-prone Louisiana coast continues at notably high rate. During the period of 1932-2010, the total land loss in coastal Louisiana was 1,833 mi^2, and the rate of loss from 1985-2010 was 16.6 mi^2/yr (Couvillion et al. 2011). This figure is often presented to the public in rather alarming terms: Louisiana is losing a football field of wetlands every hour. The reasons for wetland loss are complex and both natural and anthropogenic in origin. These include subsidence from sediment compaction and dewatering, eustatic sea-level rise, growth faults, isostatic adjustments, and erosion due to waves and storm surges. Regional anthropogenic causes include channelization of the Mississippi River, canal dredging through wetlands, and fluid withdrawal (e.g., groundwater, hydrocarbons). One of the important natural causes of coastal erosion is the constant wave action on the marsh edges. Analysis by Penland et al. (2000) shows that 26% of the wetland loss in the Mississippi River Delta from 1932 to 1990 can be attributed to erosion due to wind waves. Additionally, coastal wetlands in this region also experience frequent surge and stronger wave forces resulting from tropical storms and hurricanes. To combat the devastating wetland loss, the latest draft of Louisiana's Comprehensive Master Plan for a Sustainable Coast (CPRA 2017) has prioritized sediment diversions, shoreline protection, and marsh creation projects. In fact, marsh creation projects constitute the nation's largest investment, totaling over $20 billion, in the 2017 Draft Coastal Master Plan (CPRA 2017).

Seven predictive models were utilized to develop and assess the efficacy of the 2012 Coastal Master Plan (CPRA 2012). Among them is the Wetland Morphology Model, which forecasts the wetland changes with and without coastal protection and restoration projects in the next 50 years (Allison et al. 2015). One of the suggested improvements for the wetland morphology model is to explicitly consider marsh edge erosion and vegetation-dependent accretion in the forecast of wetland morphological changes. The rate of erosion at the marsh edge is a key parameter for predicting the longevity of a given vegetated marsh, including future marsh creation projects. The soil and plant types, along with hydrodynamic characteristics, are the controlling variables for the rate-of-retreat at marsh edges. However, there is a lack of synchronized field data of waves, currents, soil, and vegetation near a marsh edge along with understanding of the failure mechanism. Consequently, the existing capability of predicting the marsh edge erosion rate as a function of wave power, and soil and vegetation properties is rather limited. Our research group is focused on developing a robust marsh edge erosion model that

incorporates hydrodynamic, soil, and vegetation properties and is calibrated to coastal Louisiana. A more robust wetland morphology model that includes marsh edge erosion will improve our ability to forecast the impact of coastal protection and restoration projects and assist in managing of Louisiana's coastal resources.

The proposed project aims to enhance the fidelity of marsh edge erosion predictions in coastal Louisiana for improved coastal restoration and management. The major objectives are: (1) to implement a camera monitoring system to monitor horizontal evolution; and (2) to develop hypotheses of the failure mechanism of wetlands. Research has elucidated some of the key mechanisms controlling marsh edge erosion, including wind-generated waves (Chen et al. 2005; Priestas et al. 2015), presence of vegetation (D'Alpaos et al. 2007), erosion of cohesive sediment (Black et al. 2002), anthropogenic factors (Gedan et al. 2009), and soil properties (Feagin et al. 2009; Howes et al. 2010). The experimental work by Feagin et al. (2009) suggests that soil type is the primary variable that influences wave-induced erosion. Howes et al. (2010) used the shear strength of soil to explain the failure of low- and high-salinity wetlands during Hurricane Katrina. Both studies conclude that the type and properties of marsh soils are important factors to consider when comparing erosion rates among sites, yet existing prediction models for marsh stability and evolution (e.g., Schwimmer (2001) and Mariotti and Fagherazzi (2010)) predominantly focus on wave power and lump soil and vegetation effects into field-calibrated empirical constants.

Attempts to predict marsh edge retreat rate using only wave power have met varying levels of success. Schwimmer (2001) first quantified marsh boundary retreat rates in a study of various sites along Delaware's Rehoboth Bay. Retreat rates obtained by local shoreline surveys over a five-year period were used to compute the average land loss over a given shoreline length. Wind, bathymetric, and fetch data were used to hindcast the wave climate from which the total averaged wave power at each site was computed. Based on this approach, Schwimmer (2001) proposed $R = 0.35P^{1.1}$, where R is erosion rate (m/yr), P is wave power (kW/m), and 0.35 and 1.1 are field-calibrated empirical constants that account for soil type, water elevation, vegetation, and macrofauna. Similar to Schwimmer (2001), Parker (2014) analyzed aerial imagery from 1998 to 2010 to estimate the historical retreat rate of shorelines found in Terrebonne Bay. He supplemented the historical retreat rates with GPS shoreline surveys conducted over a period of 12 months and deployed wave gauges to determine the wave characteristics directly in front of the marsh edge. The recorded wave gauge data was used in Delft3D to obtain water levels in the bay, which was

then input into a SWAN model to estimate the average wave power. As a result, Parker (2014) developed Fig. 1 to relate the average wave power and retreat rates at 28 sites within Terrebonne Bay. Although retreat rates generally increase as the wave power increases (R^2 = 0.17), Fig. 1 indicates that the predictive power of erosion rate using only wave power is limited. Therefore, the inclusion of spatially varying, site-specific soil strength and vegetation in addition to the hydrodynamic driving force is a logical step towards improving a predictive model for marsh edge erosion. This project will demonstrate marsh edge erosion is a function of soil, vegetation, and wave characteristics. We hypothesize that a strong trend exists between wave energy and local site-specific erosion, but expanding from localized areas to a regional scale the magnitude of erosion likely depends on other ecological and geotechnical parameters.

2. EROSION MODELS

The marsh erosion models are divided into semi-empirical and theoretical methods, where the semi-empirical models applied to coast-wide marsh retreat predictions and theoretical models focused on individual failure events. Through this literature review, the theoretical models are further classified into limit equilibrium, laboratory derived, and field derived methods. Still, most marsh erosion models are semi-empirical, which likely results from of a lack of understanding of the progression of failure and mechanics and uncertainty in input parameters (e.g., shear strength, vegetation, hydrodynamic forcings).

The limit equilibrium method is the commonly used technique of evaluating instabilities for landslides, man-made slopes (e.g., levees, highway embankments, landfills), and riverbanks. In particular, the Bank Stability and Toe Erosion Model (BSTEM) is an approximate analogy to marsh edge erosion because, as the name suggests, it includes both stability and toe erosion. Developed at the USDA-ARS National Sedimentation Laboratory, BSTEM and its functions are discussed at length by Pollen-Whitehead and Simon (2009; 2010). The stability model can compute the factor of safety using a number of methods: horizontal layers per Simon et al. (2000), vertical slices with a tension crack per Morgenstern and Price (1965), and cantilever failures per Thorne and Tovey (1981). The model accounts for soil strength of multiple layers, partially-variable saturated soils (i.e., positive and negative pore-water pressures), confining pressure due to streamflow, and soil reinforcement and surcharge due to vegetation. The toe erosion model is

used to estimate the bank and toe erosion, which is subsequently incorporated into the stability model. The erosion is predicated on hydraulic shear stress, as determined by channel geometry, and the soil's critical shear stress and erodibility parameters. While BSTEM incorporates key parameters into its stability analysis that relate to marsh edge erosion (e.g., soil and vegetation strengths, pore-water pressures, toe erosion), there are several distinct differences between the two environments. For example, toe erosion in BSTEM is estimated from shear stress parallel to the bank, while waves breaking along a marsh edge impose perpendicular shear stresses. In addition, the dynamic impact force on the marsh bank from waves can contribute to instability through additional sediment erosion and increased pore-water pressure within the bank's constituent soil. The model assumes hydrostatic conditions and therefore does not explicitly model transient seepage. This is important to note because still water levels near marshes can vary substantially over short periods due to tides and cold fronts, whereas river levels (at a given cross-section) are relatively constant over time.

Laboratory- or field-derived models have been primarily developed for a given failure mode observed in the wave flume experiment or field. Bendoni et al. (2014) use a wave flume to replicate the toppling mass failure due to oscillating waves. They instrumented vegetated and unvegetated banks with pressure transducers, micro-tensiometers, and water content sensors to understand the dynamic soil response to waves. The governing equation for predicting failure comes by solving for the rotation of a block, which is assumed to be a rigid and impermeable body that follows viscoelastic behavior per the Kelvin-Voigt model. The failure plane is horizontal, and the failure criterion is equated to the tensile strength of the material (Fig. 1a). Hydrostatic and dynamic forcings are incorporated by estimating wave thrust and soil damping. Bendoni et al. (2014) found the conditions of (1) water inside the tension crack and (2) low water levels in front of the bank are the most unfavorable for promoting bank instability. This study indicates that the dynamic response of the system appears to be crucial in predicting bank instability, as several factors, such as elastic potential energy accumulated by the system during compression and released during the wave draw-down, and inertial effects, lead to higher stresses.

The field-derived model by Gabet (1998) replicates the undercutting failure mechanism for California estuaries. In this case, undercutting creates a cantilever soil block (Fig. 1b). This simple static model determines the moment at the end of the cantilever, where the failure criterion is determined from the driving moment of the weight of the block and soil-vegetation shear strength.

The model is used to estimate the width of undercutting before a failure occurs, which signifies lateral retreat of the marsh. Another field-derived model was proposed by Bendoni et al. (2016). In Fig. 1c, Bendoni et al. (2016) separate erosion into two layers based on the still water level and wave characteristics. In this case, soil erodibility and undercutting are incorporated into the model. If the toe face retreats at a faster rate than the top face, undercutting will form and eventually leads to a mass failure when a threshold length is exceeded. This model also accounts for the still water level. For example, the top face only erodes when the still water level is at or above the height of the toe face. In other words, the toe face will not erode if submerged and the top face will not erode if the still water level is not acting on the vertical length. The length of erosion for top and toe faces is a function of an assumed soil erodibility and wave power.

Semi-empirical models estimate marsh erosion by correlating observed retreat rates (based on aerial imagery, erosion pins, terrestrial GPS surveys, etc.) with predicted and/or measured wave characteristics. Schwimmer (2001) quantified marsh boundary retreat rates over a five-year period along sites within Rehoboth Bay, Delaware. Retreat rates obtained by local shoreline surveys were used to compute the average land loss over a given shoreline length. Wind, bathymetric, and fetch data were used to hindcast the wave climate from which the total averaged wave power at each site was computed. Based on this approach, Schwimmer (2001) proposed Eq. (H) using an empirical time-averaged erosion rate (R, m/year) as a function of wave power (P, kW/m). Marani et al. (2011) derived a linear relationship between volumetric retreat rate (V, m^2/yr) and mean wave power density (P, kg-m/yr^3) using Buckingham's theorem of dimensional analysis. The authors calibrated the average volumetric erosion rate (Eq. I) by determining the erosion rates along 150 sites inside the Venice Lagoon, Italy, using historical aerial imagery and utilizing a parametric wind model to estimate wave power. Priestas et al. (2015) used marsh retreat rates obtained from pins and shoreline surveys at 33 sites in Hog Island Bay, Virginia, to develop Eq. (J) in terms of wave power. Leonardi and Fagherazzi (2015) added an exponential function to Eq. (H) to account for variability in soil resistance (H_c) and mean wave height (H). They calibrate Eq. (K) with three sites along Plum Island Sound, Massachusetts, using the cell automata model. Mariotti and Fagherazzi (2010) developed an eco-geomorphic model to study the long-term evolution of salt marshes. To replicate marsh erosion, they emulated the formula for mud erosion, $R = \alpha(\tau - \tau_c)$, by including a critical wave power threshold (P_{cr}) and empirical constant (β) calibrated to produce retreat rates in practical units (i.e., m/yr). Because this study investigated hypothetical cases, the

model (Eq. L) was not validated against field or laboratory data.

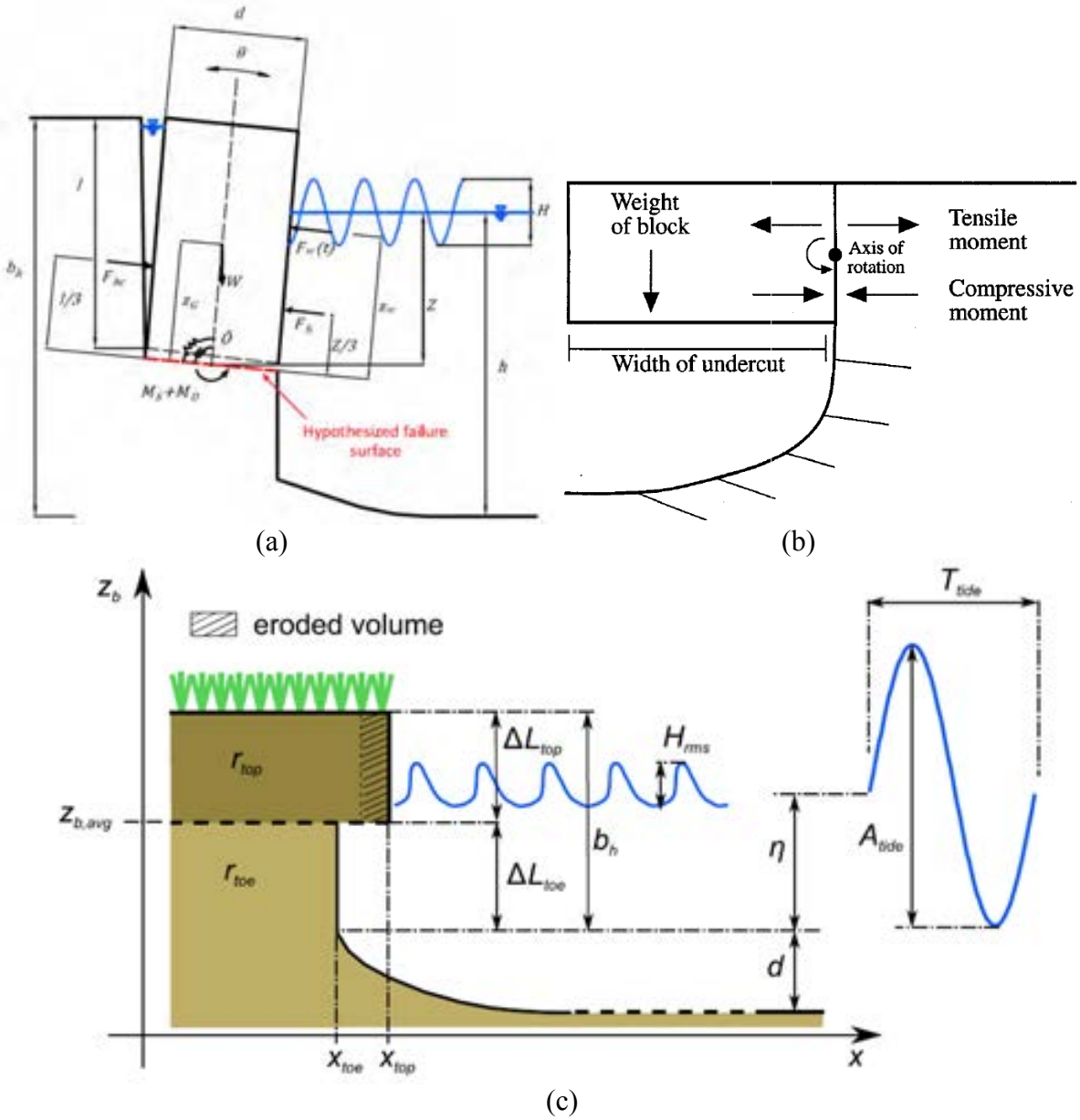

Fig. 1. Examples of theoretical models: (a) Bendoni et al.'s (2014) toppling mass failure showing forces acting on a rigid block, (b) Gabet's (1998) undercutting formulation using moment of cantilever, (c) Bendoni et al.'s (2016) field-based erodibility of two layers and undercutting-of-mass failures

Table 3. Summary of semi-empirical marsh erosion models

Study	Model Equation		Parameters
Schwimmer (2001)[a]	$R = 0.35P^{1.1}$	(H)	▪ R (m/yr): local shoreline surveys ▪ P (kW/yr): average wave power, hindcast from historical wind, bathymetric, and fetch data
Marani et al. (2011)[b]	$V = 0.03P + 0.19$	(I)	▪ V (m^2/yr): historical imagery, assumed scarp height ▪ P (kg-m/yr^3): parametric wind model
Priestas et al. (2015)[c]	$R = 0.079P + 0.43$	(J)	▪ R (m/yr): pin and shoreline surveys ▪ P (kW/m): SWAN
Leonardi and Fagherazzi (2015)[d]	$R = 0.35P^{1.1}\exp\left(-\frac{H_c}{H}\right)$	(K)	▪ R (m/yr): GPS surveys ▪ P (kW/m): per Young and Verhagen (1996) ▪ H_c (m): equal to $4 \cdot S_u/\gamma$ ▪ S_u (kPa): measured by vane shear apparatus ▪ γ (kN/m^3): saturated unit weight ▪ H (m): mean wave height
Mariotti and Fagherazzi (2010)[e]	$R = \beta\left(P - P_{cr}\right)$	(L)	▪ β: empirical factor ▪ P: per linear wave theory ▪ P_{cr}: critical wave power, a function of biomass

[a] Based on surveys of Rehoboth Bay, DE
[b] Based on surveys of Venice Lagoon, Italy
[c] Based on surveys of Hog Island Bay, VA
[d] Based on surveys of Plum Island Sound, MA
[e] Based on a hypothetical location

Recent attempts to develop theoretical and empirical marsh-edge retreat rate models have met varying levels of success. This may be due to several reasons, including a lack of knowledge of the mobilized failure mode and corresponding mechanistic formulations, missing input parameters (e.g., geotechnical, ecological, marsh profile), and temporal incompatibility. The theoretical models discussed herein (Bendoni et al. 2014; Bendoni et al. 2016; Gabet 1998) capture two failure modes (undercutting and soil erodibility) at varying degrees of complexity. These models highlight the need to account for the failure mode, as undercutting failure is found to control the retreat rate. The simplistic nature of each model stems from insufficient observations of the progression of failure in the field. The long-term goal of the theoretical models is to achieve a level of sophistication similar to that of BSTEM and geotechnical slope stability models based on limit equilibrium or finite element methods. Johnson (2016) represent the first models to incorporate shear strength in their formulations. The marsh profile can also play an influential role; for example, the marsh platform and mudflat elevations control the wave power estimates. Thus, an area of future research is developing models that include geotechnics (shear strength, wave damping), ecology (vegetation type, roots), and marsh profile in the semi-empirical models.

Bendoni et al. (2016) compared short-term (weeks to months) to long-term (years to decades) retreat rates reported by Marani et al. (2011) and found the short-term rates to be much greater. They explained this observation using the analogy to the dependence of the rate of bed load transport on sampling frequency described by Singh et al. (2009). Longer time scale observations tend to smooth out higher peak fluctuations and include both variations intrinsic to the physical processes at work and possible changes in external forcing (e.g., variation due to human activities or climate change). As a result, these findings suggest there is an important need to develop process-based, mechanistic models for investigating possible long-term evolution of marshes by carrying out field observations on short time scales.

3. SITE INVESTIGATION

Fig. 2 shows an overview of Terrebonne Bay, Louisiana, and the camera monitoring site. The investigations in this area began about 10 years ago by Kyle Parker, a Master's student in Professor Q. Jim Chen's research group. Prior work focused on RTK measurements of the shoreline erosion rate and waves impacting the marsh edge. The site has historically experienced high erosion rates of several meters per year.

The majority of wetland monitoring sites focus on vertical evolution of marshes (Temmerman et al., 2003; Kirwan and Murray, 2007), while only few studies have continuously observed the horizontal evolution of coastal marshes. As a result, the specific mechanisms and causes of marsh retreat via mass failures and particle-by-particle erosion due to wind waves are not well identified (Gabet, 1998; Schwimmer, 2001; Gedan et al., 2009; Marani et al., 2011). While there are an increasing number of studies using physical experiments for simulating marsh environments (e.g., Coops et al., 1996; Chen et al., 2013; Feagin et al., 2009; Francalanci et al., 2015; Bendoni et al., 2015), a potential drawback of the small-scale physical models is the temporal incompatibility, i.e., the experiment duration is much shorter than processes in the field. Field reconnaissance of coastal marsh erosion is predominantly focused on measuring boundary retreat rates from aerial imagery, total station and prism rod, GPS units, and erosion pins. The site visits are also spaced 3 to 4 months apart, so extensive monitoring to identify the progression of marsh failure is not feasible. Time-lapse still and motion imagery include a wealth of visible details for the observation of soil behavior, infrequent and extreme events in ecology, geology, and meteorology (Newbery and Southwell, 2009; Holman et al., 2003). For example, Zhang et al.

(2014) installed low power and low cost networked smart cameras to document the short-term processes of bluff erosion. This work involved leveraging archived images to visualize and characterize the evolution of marsh edge erosion. We are exploring four important questions regarding the progression of marsh edge erosion: (1) What is the failure mechanism; (2) How rapidly is erosion occurring; (3) Is the erosion chronic or episodic; and (4) Is it linked to any predictable physical or meteorological event?

Fig. 2. Overview of camera site in Terrebonne Bay near Cocodrie, LA and LUMCON (image courtesy of Google)

3.2 Time-Lapse Camera

Although laboratory and field observations suggest three marsh edge erosion mechanisms are prevalent (slumping, undercutting, and root scalping), long-term continuous monitoring has not been performed to understand the time-dependent erosion process. As a result, we installed 4 Moultrie Outdoor cameras (encased in weather-resistant housing) to identify the progression of marsh erosion using time-lapse imaging. The camera was mounted on an open-ended steel pipe that was driven sufficiently into the ground to provide an adequate foundation capable of resisting wave and wind forces (Fig. 3). The camera is angled at an oblique view to the shoreline to monitor

the waves impacting the marsh edge. The photos will be collected on a subsequent field trip and analyzed for developing a framework for the progression of marsh edge erosion. The cameras are currently recording images since April 2017. The April 2017 photos were obtained using Brinno construction cameras. We found that the image quality and reliability were low for our applications in the wetlands. The August 2017 field campaign replaced the Brinno cameras with the Moultrie cameras. They record data using 32 GB scandisks and 12 AAA batteries. This hard drive battery power typically lasts about 3 months. Erosion pins and markers were also installed in August 2018 to quantify the local shoreline erosion. The subsequent field investigation in November 2017 collected images from August to November 2017 for analysis.

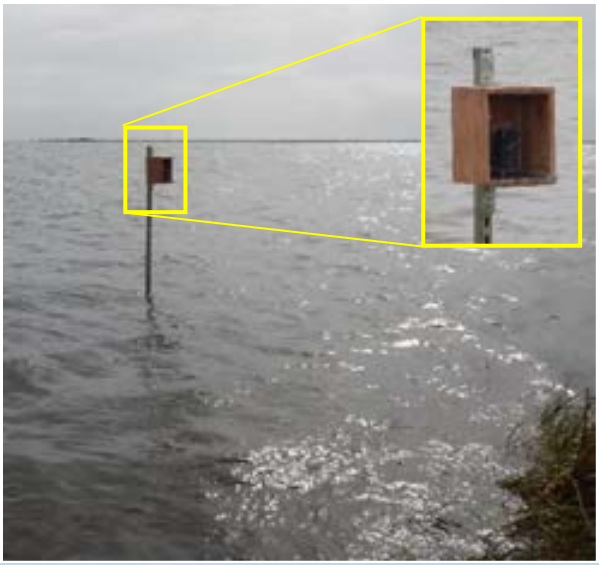

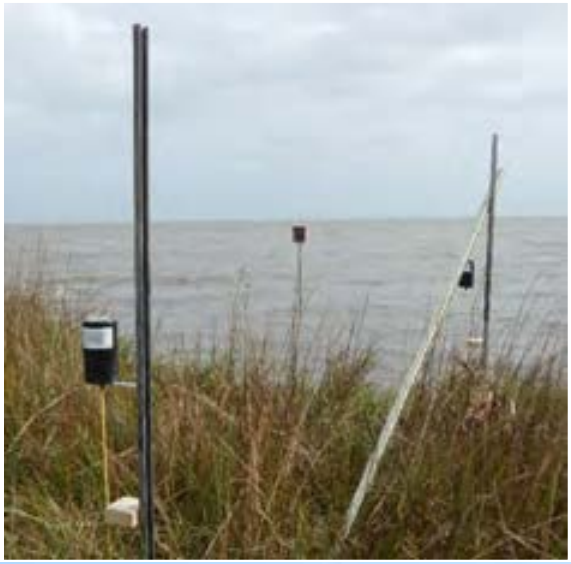

Fig. 3. Time-lapse camera after installation

4. RESULTS

This section provides the preliminary results for the camera monitoring system. In particular, select images are provided herein. Appendix A provides a prepared presentation that provides a qualitative assessment of the cameras. Overall, three cameras recorded from August 18, 2017 to November 18, 2017. Images were taken every 10 minutes from 6:00 AM to 5:50 PM. Two major storm events were observed on August 29 and August 30. After these events, the vegetation was noticeably less dense. The force from these major events We are attempting to quantify how much vegetation was lost using the cameras. Shoreline erosion was qualitatively monitored using markers and erosion pins. Rate was more or less "constant", meaning major events did not lead to significant erosion although not all major events were likely captured. Smaller events gradually erode the "organic muck" below and between the vegetation (i.e., undercutting). Major events likely erodes some mudflat but more importantly removes vegetation which destabilizes the soil.

Fig. 3. Erosion rates determine from the erosion pins from April to August 2017

MOULTRIE
33°C 30.06inHg
JAFARI-B-CAM
18 AUG 2017 02:00 pm

MOULTRIE
25°C 29.79inHg
JAFARI-B-CAM
29 AUG 2017 07:20 am

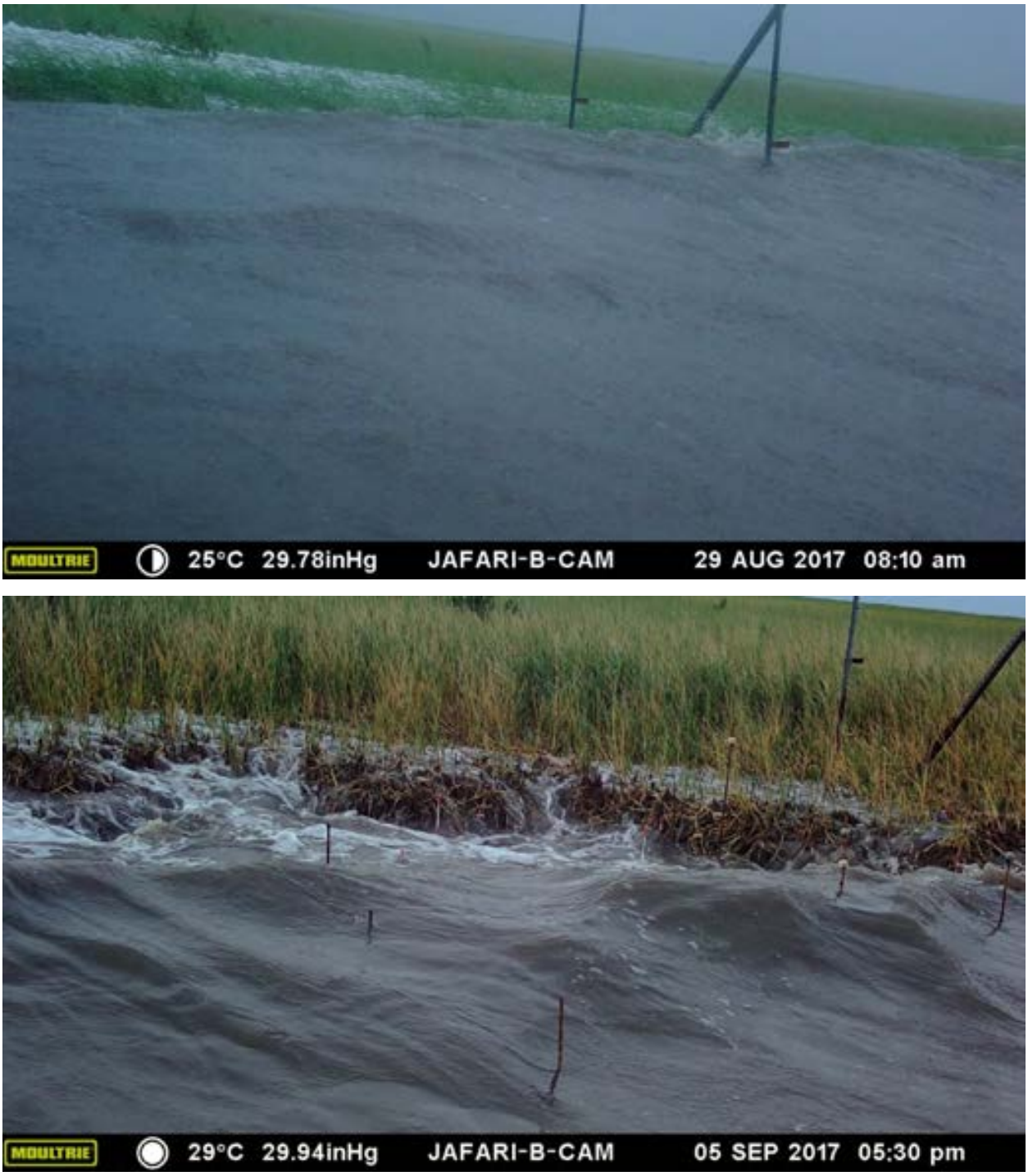

Fig. 4. Select images from relatively major and minor storm

6. CONCLUSIONS

The draft of Louisiana's 2017 Coastal Master Plan (CPRA) estimates that up to an additional 1,756 m^2 of land will be lost in the next 50 years without aggressive coastal restoration and protection.

A major mechanism causing a large proportion of the observed land loss is wind waves and surges attacking marsh boundaries. This process spurs a positive feedback cycle by increasing fetch and depth in a shallow coastal waterbody. This scenario is rapidly increasing rates of marsh edge erosion in Terrebonne Bay, Barataria Bay, and Breton Sound, Louisiana (Chen et al. 2013). Therefore, a model that can confidently predict the response of a stretch of coastal marsh to a given wave climate would prove a valuable tool for the management of coastal resources to mitigate erosion hazards.

REFERENCES

Allison, M., Chen, Q. J., Couvillion, B., Freeman, A., Leadon, M., McCorquidale, A., Meselhe, E., Ramatchandirane, C., Reed, D., and White, E. (2015). "2017 Coastal Master Plan: Model Improvement Plan, Attachment C3-2 – Marsh Edge Erosion." *2017 Draft Coastal Master Plan*, Coastal Protection and Restoration Authority, Baton Rouge, LA, 51.

American Society for Testing and Materials (2012). "Electronic friction cone and piezocone penetration testing of soils." *D5778*, ASTM International, West Conshohocken, PA.

American Society for Testing and Materials (2015). "Field vane shear test in saturated fine-grained soils." *D2573/D2573M*, ASTM International, West Conshohocken, PA.

Amos, C. L., Grant, J., Daborn, G. R., and Black, K. (1992). "Sea Carousel—A benthic, annular flume." *Estuarine, Coastal and Shelf Science*, 34(6), 557-577.

Are, D., Kemp, G. P., Giustina, F., Day, J., and Scarton, F. (2002). "A portable, electrically-driven Dutch cone penetrometer for geotechnical measurements in soft estuarine sediments." *Journal of Coastal Research*, 18(2), 372-378.

ASTM (2014). "Standard practices for preserving and transporting soil samples." *D4220/D4220M*, ASTM International,, West Conshohocken, PA.

Bendoni, M., Francalanci, S., Cappietti, L., and Solari, L. (2014). "On salt marshes retreat: Experiments and modeling toppling failures induced by wind waves." *J. Geophys. Res.*, 119(3), 603-620.

Bendoni, M., Mel, R., Solari, L., Lanzoni, S., Francalanci, S., and Oumeraci, H. (2016). "Insights into lateral marsh retreat mechanism through localized field measurements." *Water Resour. Res.*, 52(2), 1146-1464.

Black, K., Tolhurst, T. J., Paterson, D. M., and Hagerthey, S. E. (2002). "Working with natural cohesive sediments." *Journal of Hydraulic Engineering*, 128(1), 2-8.

Briaud, J.-L., Li, Y., and Rhee, K. (2006). "BCD: A soil modulus device for compaction control." *Journal of Geotechnical and Geoenvironmental Engineering*, 132(1), 108-115.

Chen, Q., Ozeren, Y., Zhang, G., Wren, D., Wu, W., Jadhav, R., Parker, K., and Pant, H. (2013). "Laboratory and field investigations of marsh edge erosion." *Sediment Transport: Monitoring, Modeling and Management*, A. A. Khan, and W. Wu, eds., Nova Science Publishers, 311-337.

Chen, Q., Zhao, H., Hu, K., and Douglass, S. L. (2005). "Prediction of wind waves in a shallow estuary." *Journal of Waterway, Port, Coastal, and Ocean Engineering*, 131(4), 137-148.

Couvillion, B. R., Barras, J. A., Steyer, G. D., Sleavin, W., Fischer, M., Beck, H., Trahan, N., Griffin, B., and Heckman, D. (2011). "Land area change in coastal Louisiana from 1932 to 2010." *National Wetlands Research Center*, USGS, Lafayette, LA.

CPRA (2012). *2012 Coastal Master Plan*, Coastal Protection and Restoration Authority, Baton Rouge, LA.

CPRA (2015). *Louisiana Flood Protection Design Guidelines (LFPDG) – Geotechnical Section*, Coastal Protection and Restoration Authority, Baton Rouge, LA.

CPRA (2017). *2017 Draft Coastal Master Plan*, Coastal Protection and Restoration Authority, Baton Rouge, LA.

CPRA (2017). "Coastwide Reference Monitoring System-Wetlands Monitoring Data."Baton Rouge, LA.

D'Alpaos, A., Lanzoni, S., Marani, M., and Rinaldo, A. (2007). "Landscape evolution in tidal embayments: Modeling the interplay of erosion, sedimentation, and vegetation dynamics." *Journal of Geophysical Research*, 112(F1).

Day, J. W., Kemp, G. P., Reed, D. J., Cahoon, D. R., Boumans, R. M., Suhayda, J. M., and Gambrell, R. (2011). "Vegetation death and rapid loss of surface elevation in two contrasting Mississippi Delta salt marshes: The role of sedimentation, autocompaction and sea-level rise." *Ecol. Eng.*, 37(2), 229-240.

Feagin, R. A., Lozada-Bernard, S. M., Ravens, T. M., Möller, I., Yeager, K. M., and Baird, A. H. (2009). "Does vegetation prevent wave erosion of salt marsh edges?" *Proc. Natl. Acad. Sci. U.S.A.*, 106(25), 10109-10113.

Gabet, E. J. (1998). "Lateral migration and bank erosion in a saltmarsh tidal channel in San Francisco Bay, California." *Estuaries*, 21(4), 745-753.

Gedan, K. B., Silliman, B. R., and Bertness, M. D. (2009). "Centuries of human-driven change in salt marsh ecosystems." *Ann Rev Mar Sci*, 1, 117-141.

Howes, N. C., FitzGerald, D. M., Hughes, Z. J., Georgiou, I. Y., Kulp, M. A., Miner, M. D., Smith, J. M., and Barras, J. A. (2010). "Hurricane-induced failure of low salinity wetlands." *Proc. Natl. Acad. Sci. U.S.A.*, 107(32), 14014-14019.

Johnson, C. L. (2016). "The influence of soil properties on marsh edge erosion." M.S.C.E. master's thesis, Louisiana State Univ., Baton Rouge, LA.

Knutson, P. L. (1987). "Role of coastal marshes in energy dissipation and shore protection." *The Ecology and Management of Wetlands*, D. D. Hook, W. H. McKee, Jr., H. K. Smith, J. Gregory, V. G. Burrell, Jr., M. R. DeVoe, R. E. Sojka, S. Gilbert, R. Banks, L. H. Stolzy, C. Brooks, T. D. Matthews, and T. H. Shear, eds., Timber Press, Portland, OR, 161-175.

Leonardi, N., and Fagherazzi, S. (2015). "Effect of local variability in erosional resistance on large scale morphodynamic response of salt marshes to wind waves and extreme events." *Geophysical Research Letters*, 42(14), 5872-5879.

Lo, E. L., Bentley, S. J., and Xu, K. (2014). "Experimental study of cohesive sediment consolidation and resuspension identifies approaches for coastal restoration: Lake Lery, Louisiana." *Geo-Marine Letters*, 34(6), 499-509.

Marani, M., D'Alpaos, A., Lanzoni, S., and Santalucia, M. (2011). "Understanding and predicting wave erosion of marsh edges." *Geophysical Research Letters*, 38(21), L21401.

Mariotti, G., and Fagherazzi, S. (2010). "A numerical model for the coupled long-term evolution of salt marshes and tidal flats." *Journal of Geophysical Research*, 115(F1).

Morgenstern, N. R., and Price, V. E. (1965). "The analysis of the stability of general slip surface." *Géotechnique*, 15(1), 79-93.

Parker, K. R. (2014). "Field and numerical investigation of wave power and shoreline retreat in Terrebonne Bay, Southern Louisiana." M.S.C.E. master's thesis, Louisiana State Univ., Baton Rouge, LA.

Penland, S., Wayne, L., Britsch, L. D., Williams, S. J., Beall, A. D., and Butterworth, V. C. (2000). "Process classification of coastal land loss between 1932 and 1990 in the

Mississippi River Delta Plain, Southeastern Louisiana." U.S. Geological Survey, Woods Hole, MA.

Pestrong, R. (1972). "Tidal-flat sedimentation at Cooley Landing, Southwest San Francisco Bay." *Sediment. Geol.*, 8(4), 251-288.

Pollen-Bankhead, N., and Simon, A. (2009). "Enhanced application of root-reinforcement algorithms for bank-stability modeling." *Earth Surface Processes and Landforms*, 34(4), 471-480.

Pollen-Bankhead, N., and Simon, A. (2010). "Hydrologic and hydraulic effects of riparian root networks on streambank stability: Is mechanical root-reinforcement the whole story?" *Geomorphology*, 116(3-4), 353-362.

Priestas, A., Mariotti, G., Leonardi, N., and Fagherazzi, S. (2015). "Coupled Wave Energy and Erosion Dynamics along a Salt Marsh Boundary, Hog Island Bay, Virginia, USA." *Journal of Marine Science and Engineering*, 3(3), 1041-1065.

Redfield, A. C. (1972). "Development of a New England salt marsh." *Ecol. Monogr.*, 42(2), 201-237.

Robertson, P. K. (2009). "Interpretation of cone penetration tests – A unified approach." *Canadian Geotechnical Journal*, 14(4), 465-481.

Sasser, C. E., Evers-Hebert, E., Milan, B., and Holm, G. O., Jr. (2013). "Relationships of marsh soil strength to vegetation biomass." Coastal Protection and Restoration Authority, Baton Rouge, LA, 73.

Schwimmer, R. A. (2001). "Rates and processes of marsh shoreline erosion in Rehoboth Bay, Deleware, U.S.A." *Journal of Coastal Research*, 17(3), 672-683.

Simon, A., Curini, A., Darby, S. E., and Langendoen, E. J. (2000). "Bank and near-bank processes in an incised channel." *Geomorphology*, 35(3-4), 193-217.

Singh, A., Fienberg, K., Jerolmack, D. J., Marr, J., and Foufoula-Georgiou, E. (2009). "Experimental evidence for statistical scaling and intermittency in sediment transport rates." *Journal of Geophysical Research*, 114(F1), F01025.

Thorne, C. R., and Tovey, N. K. (1981). "Stability of composite river banks." *Earth Surface Processes and Landforms*, 6(5), 469-484.

Topp, G. C., Davis, J. L., and Annan, A. P. (1980). "Electromagnetic determination of soil water content: Measurements in coaxial transmission lines." *Water Resour. Res.*, 16(3), 574-582.

Turner, R. E. (2010). "Beneath the salt marsh canopy: Loss of soil strength with increasing nutrient loads." *Estuaries and Coasts*, 34(5), 1084-1093.

Wilson, C. A., and Allison, M. A. (2008). "An equilibrium profile model for retreating marsh shorelines in southeast Louisiana." *Estuarine, Coastal and Shelf Science*, 80(4), 483-494.

Wilson, C. A., Hughes, Z. J., and Fitzgerald, D. M. (2012). "The effects of crab bioturbation on Mid-Atlantic saltmarsh tidal creek extension: Geotechnical and geochemical changes." *Estuarine, Coastal and Shelf Science*, 106, 33-44.

Young, I. R., and Verhagen, L. A. (1996). "The growth of fetch limited waves in water of finite depth. Part 1. Total energy and peak frequency." *Coastal Engineering*, 29(1-2), 47-78.

Appendix A
Marsh Edge Erosion Camera Monitoring System

Brendan Copley & Navid H. Jafari

Dept. of Civil & Environmental Engineering

February 28, 2018

Sea Grant Louisiana

LSU

Summary of Camera Monitoring System

- Three cameras recorded from August 18, 2017 to November 18, 2017. Images were taken every 10 minutes from 6:00 AM to 5:50 PM.
- Photos reviewed = 3 cameras x 72 photos/day/camera x 90 days = 19,440
- "Major" storm events on August 29 and August 30, with some "smaller" events (e.g., September 5). Smaller events defined as less than 0.5 m above marsh surface elevation.
- Vegetation was noticeably less dense (i.e., thinner) after major storm events. Recovery of vegetation still ongoing (?).
- Shoreline erosion was qualitatively monitored using markers and erosion pins. Rate was more or less "constant", meaning major events did not lead to significant erosion although not all major events were likely captured.
- Preliminary erosion mechanism: Smaller events gradually erode the "organic muck" below and between the vegetation (i.e., undercutting). Major events likely erodes some mudflat but more importantly removes vegetation which destabilizes the soil.
- Next steps: (1) Photogrammetric analyses to determine erosion rates; (2) Analyze next set of photos (November 18, 2017 to present).

Time-lapse Imagery of Marsh Edge Erosion

Field Installation (August 17, 2017)

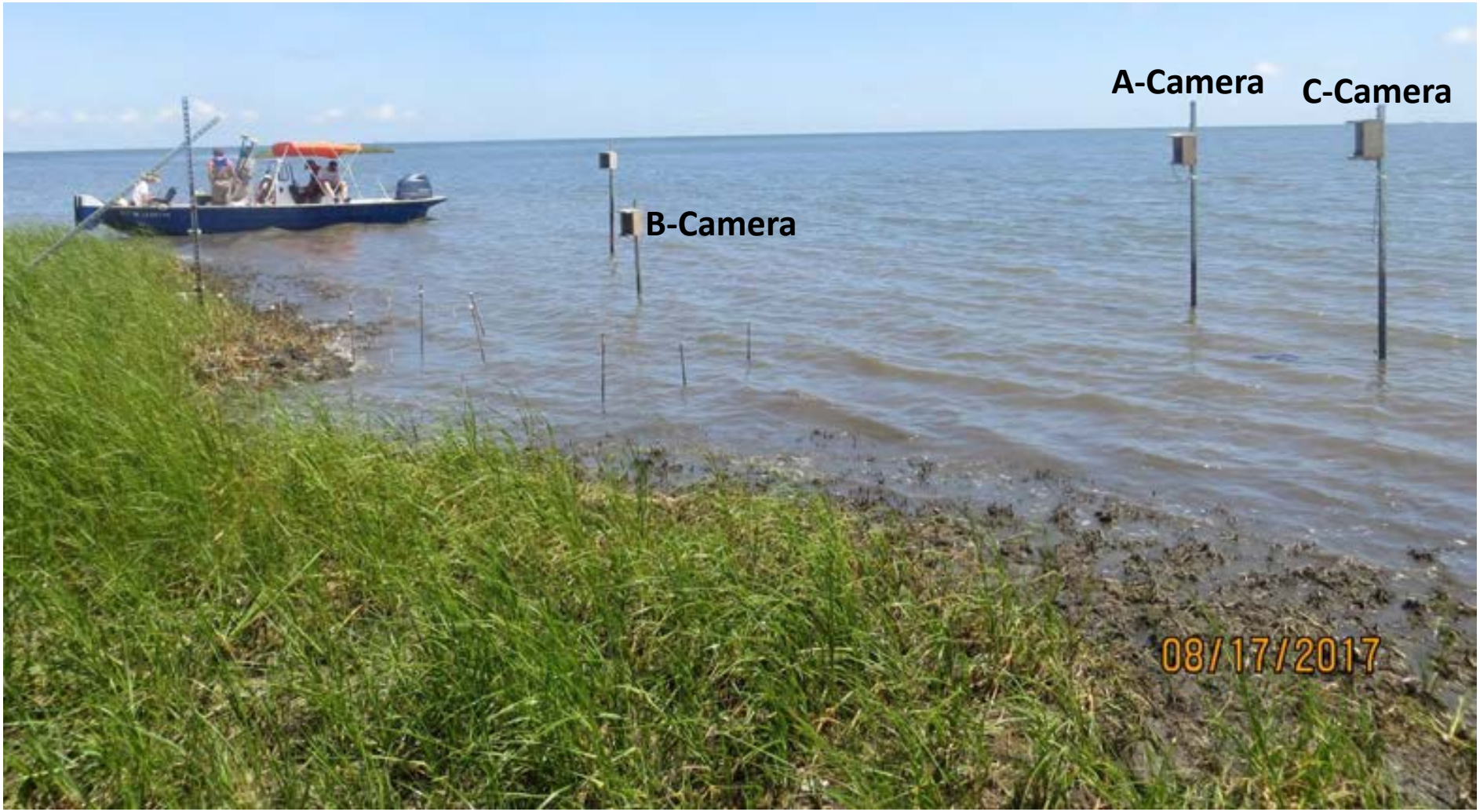

Camera B Time Lapse Photos

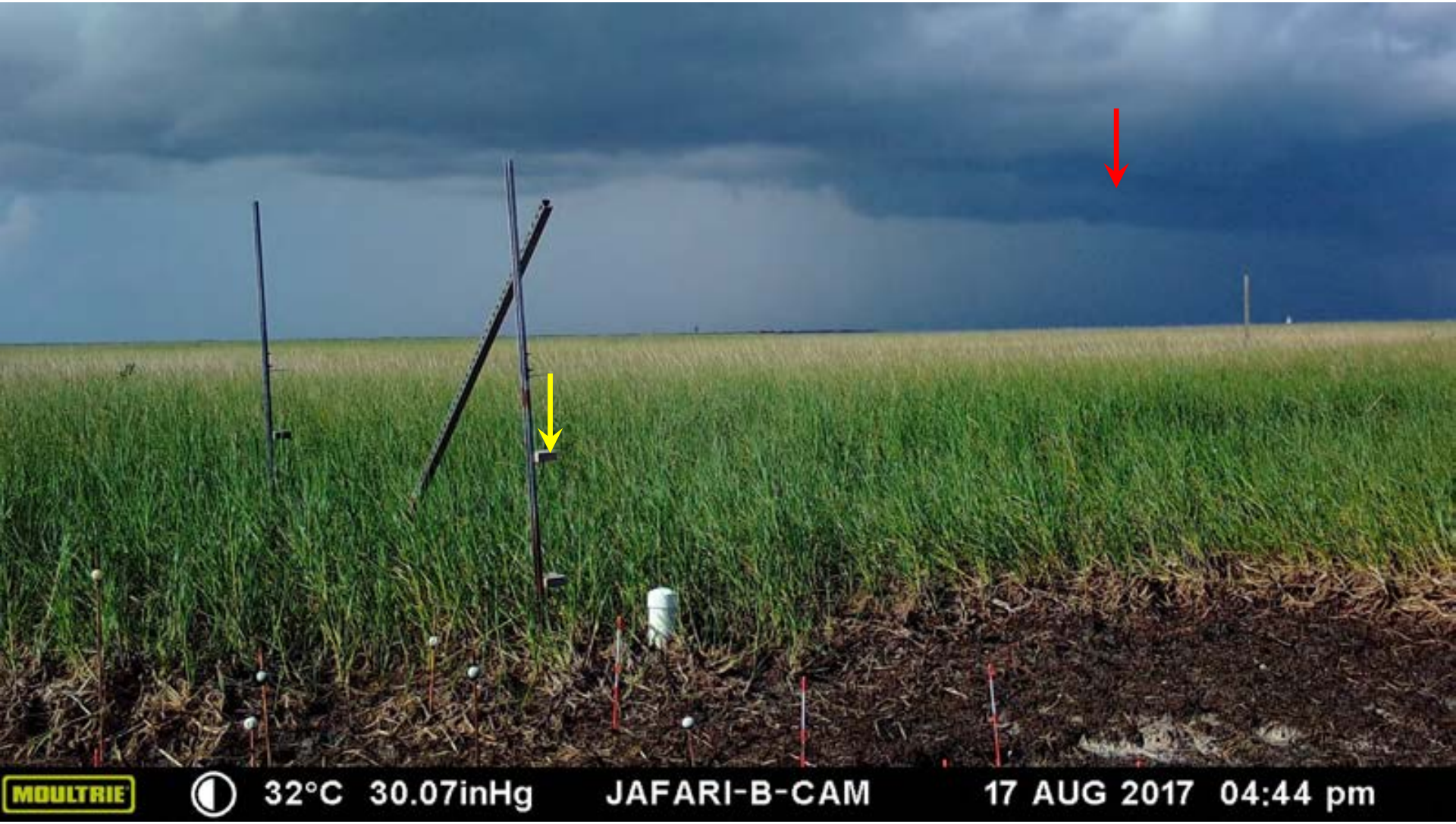

Camera B Time Lapse Photos

Camera B Time Lapse Photos

Camera B Time Lapse Photos

Camera B Time Lapse Photos

Camera B Time Lapse Photos

Camera B Time Lapse Photos

Camera B Time Lapse Photos

Camera B Time Lapse Photos

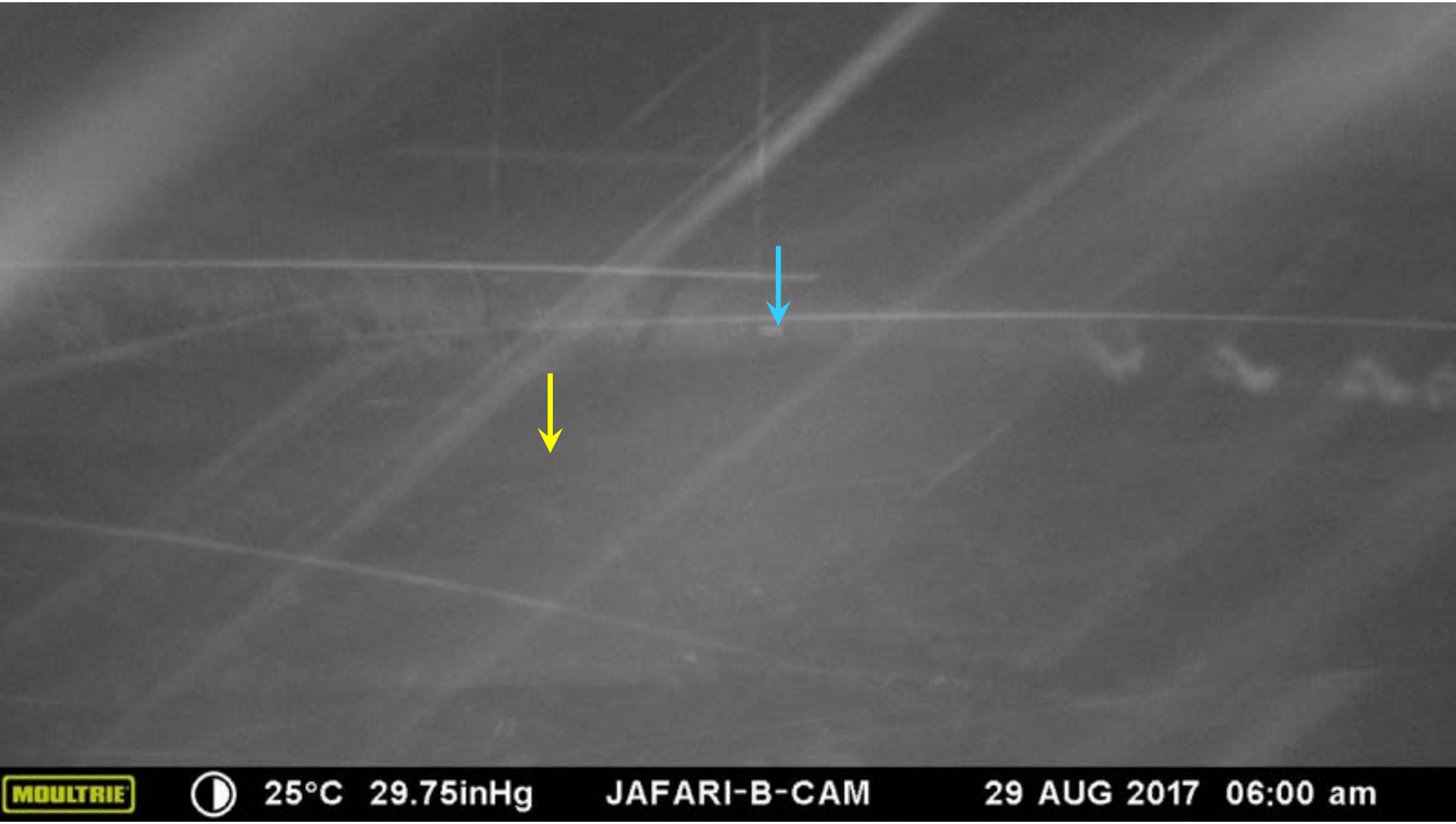

Camera B Time Lapse Photos

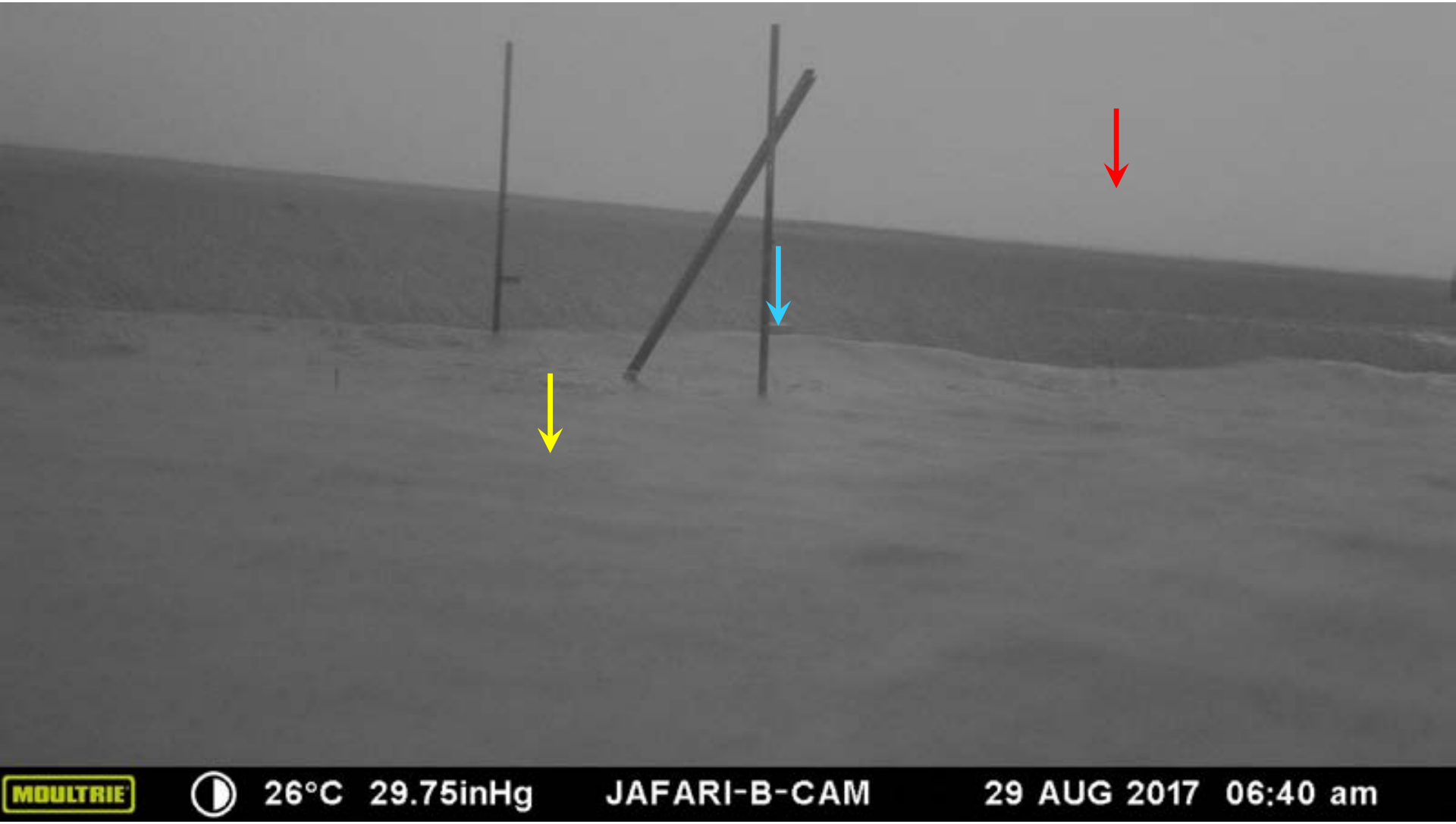

Camera B Time Lapse Photos

Camera B Time Lapse Photos

Camera B Time Lapse Photos

Camera B Time Lapse Photos

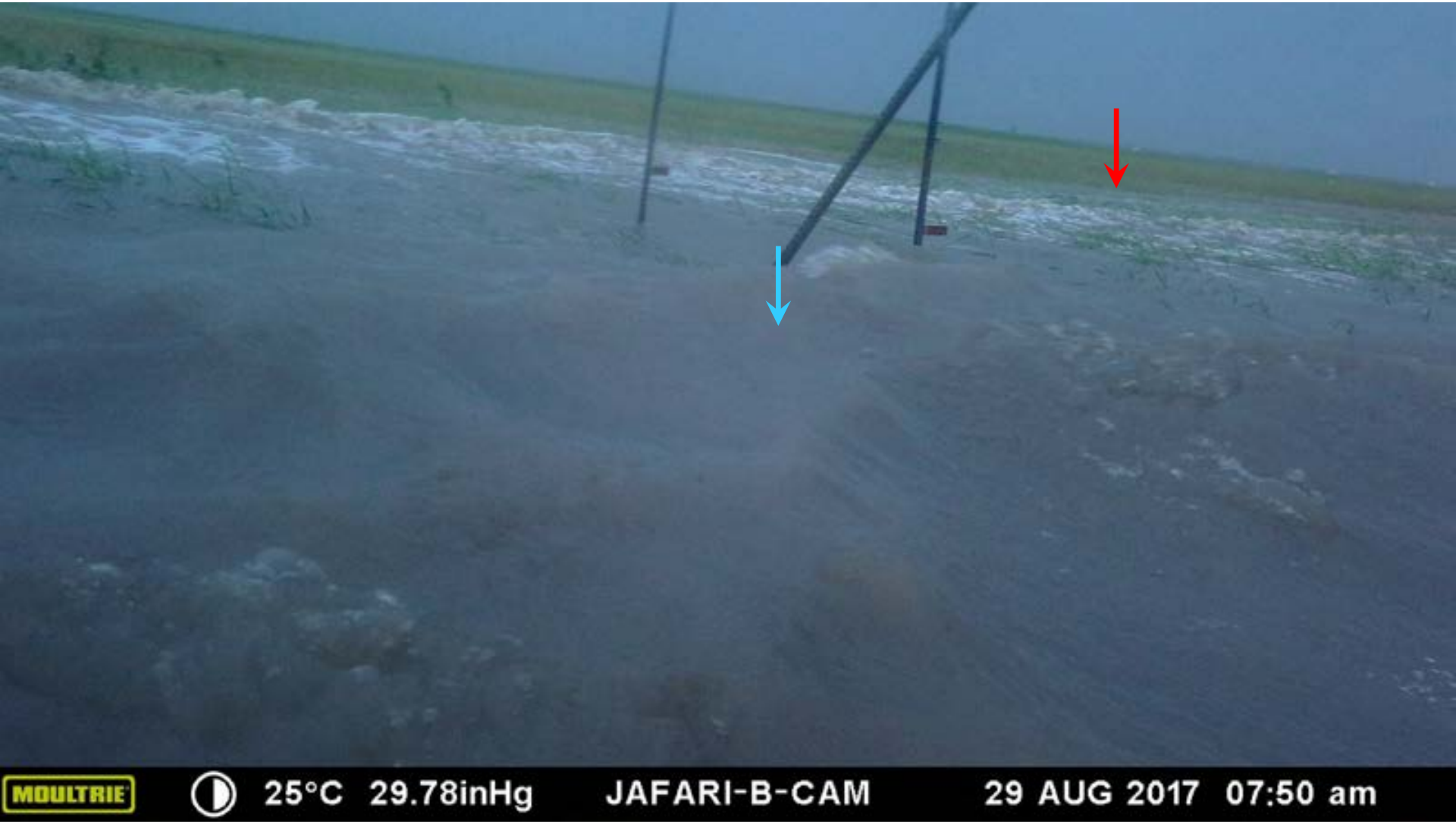

Camera B Time Lapse Photos

Camera B Time Lapse Photos

Camera B Time Lapse Photos

Camera B Time Lapse Photos

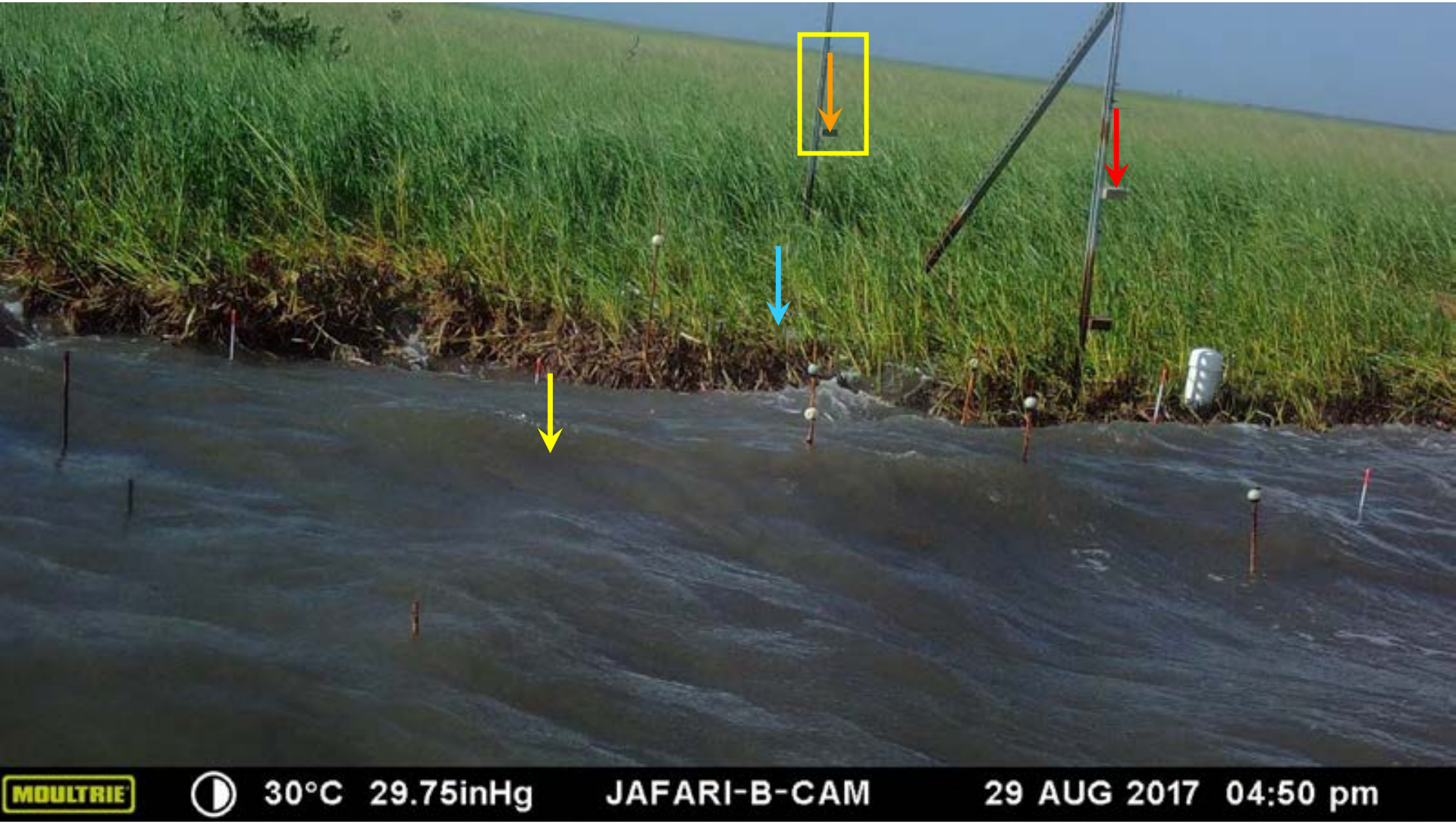

Camera B Time Lapse Photos

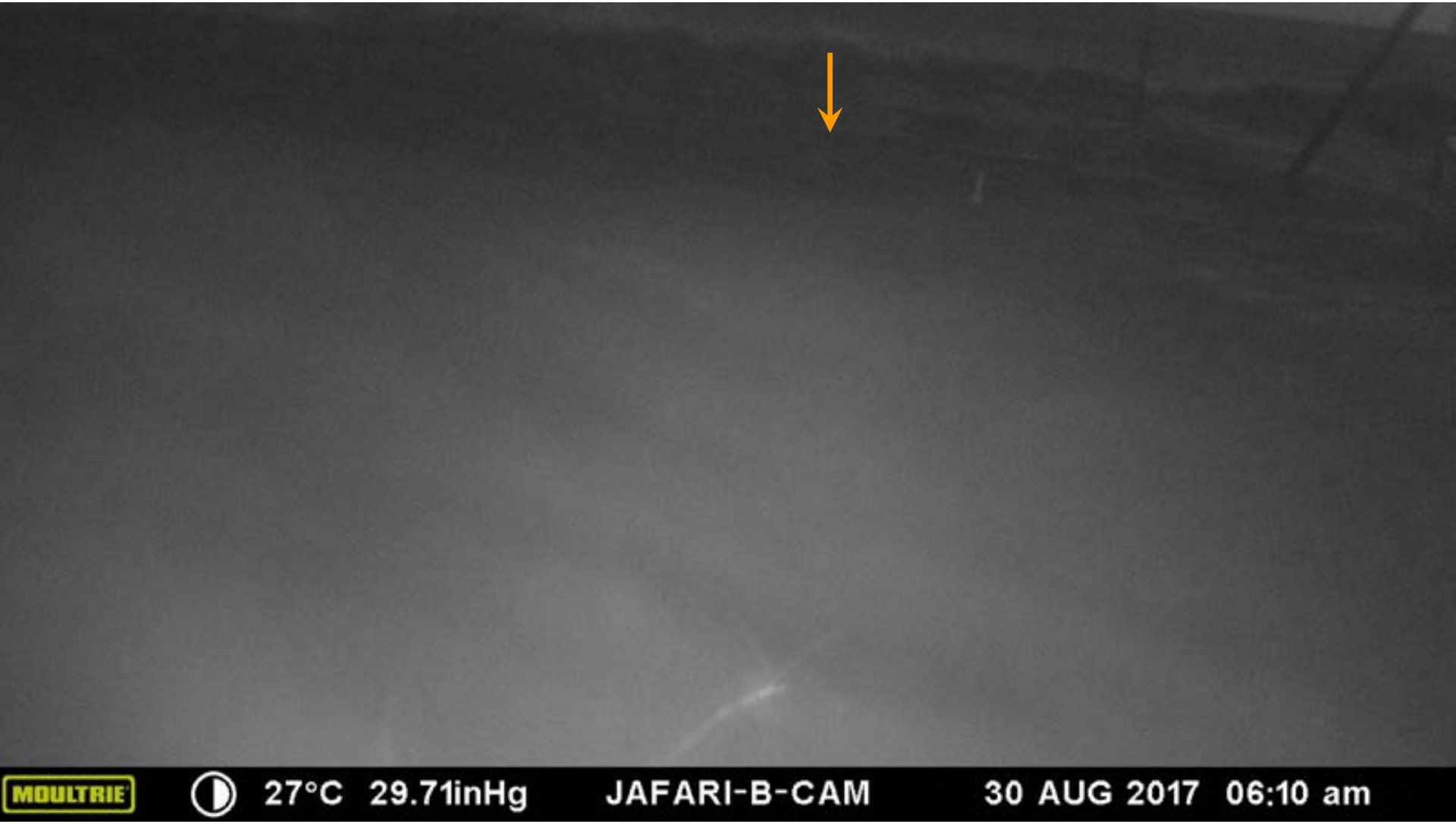

Camera B Time Lapse Photos

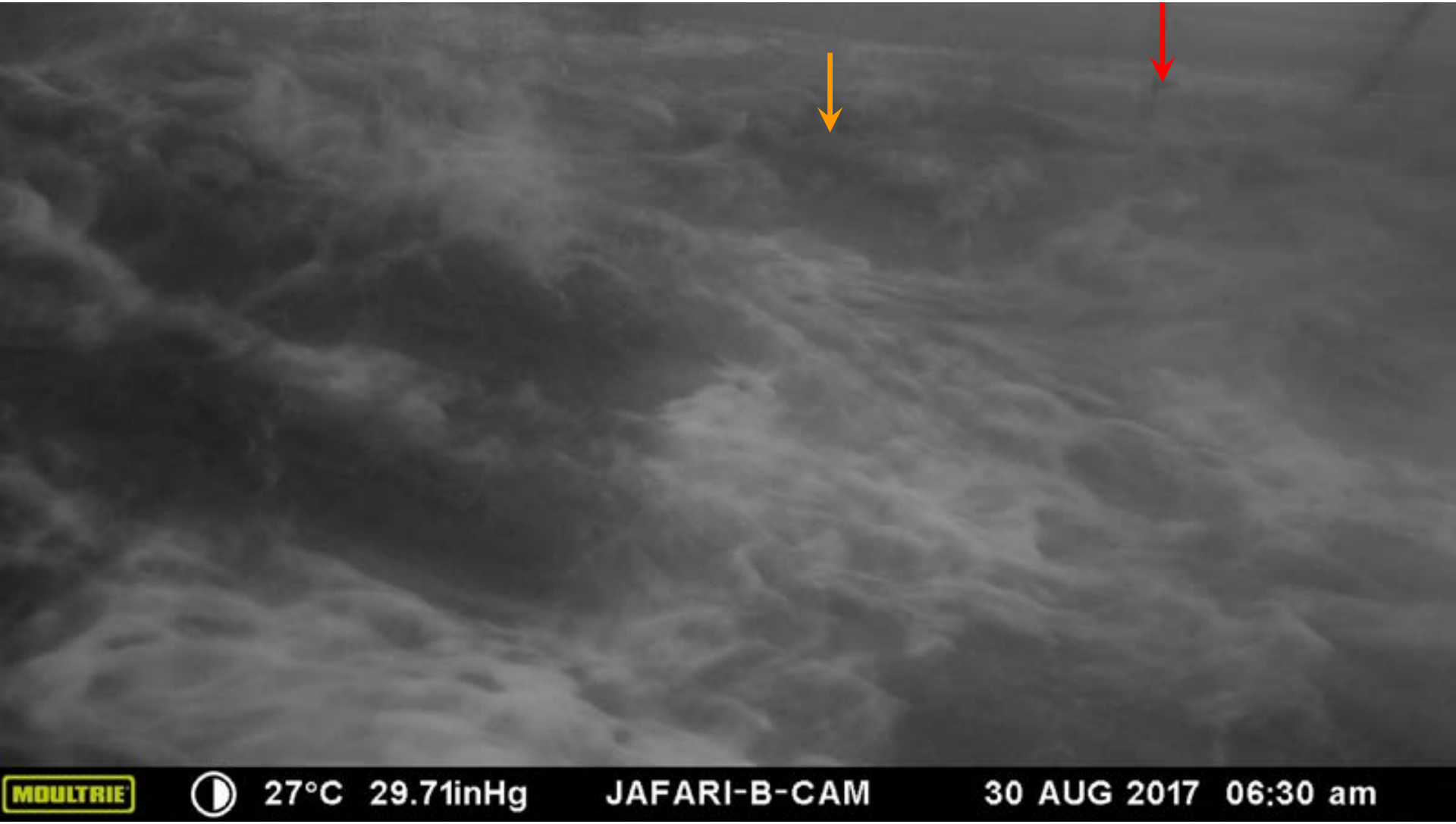

Camera B Time Lapse Photos

Camera B Time Lapse Photos

Vegetation Removed → Compare to Next Slide

Camera B Time Lapse Photos

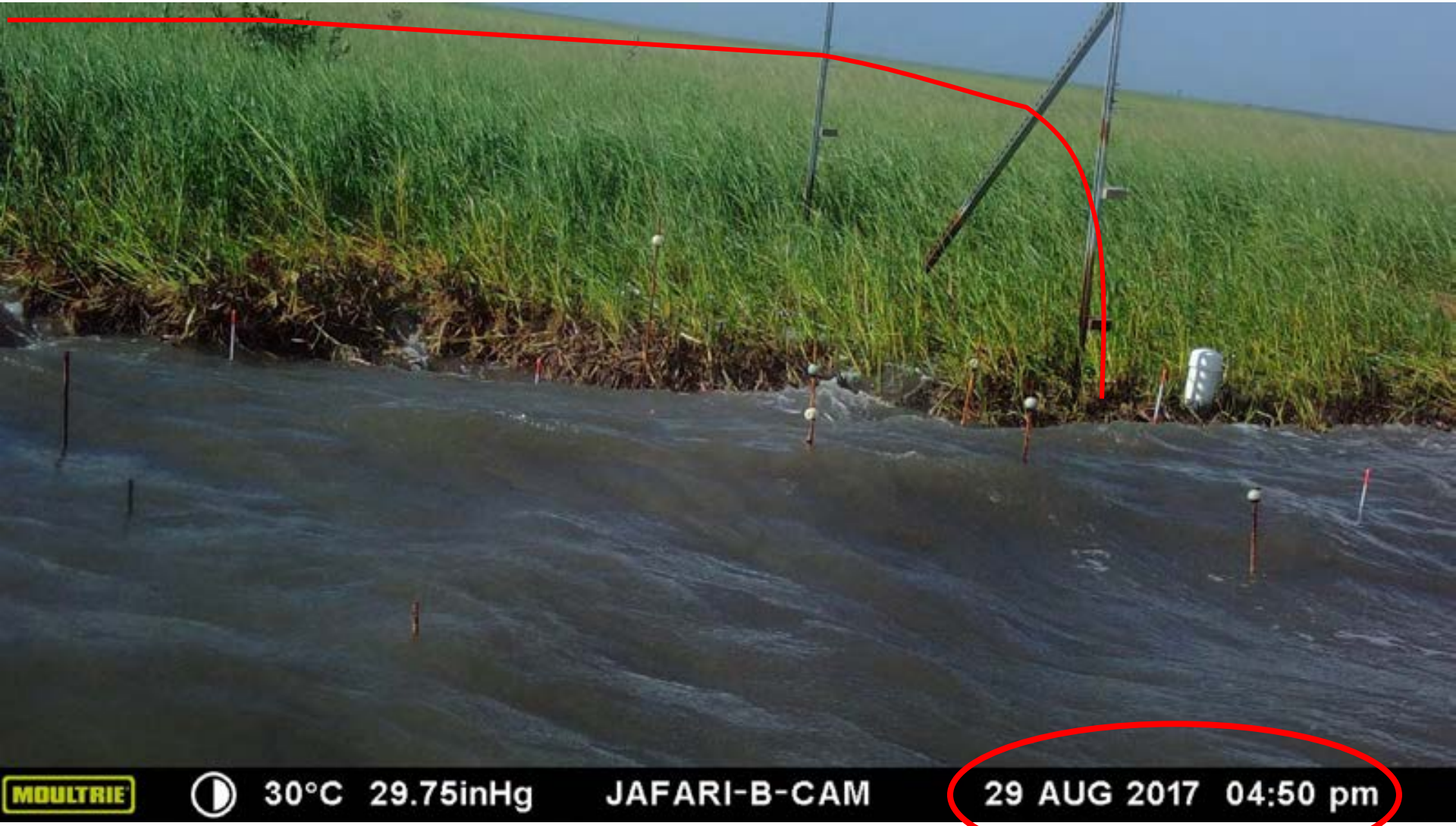

Camera B Time Lapse Photos

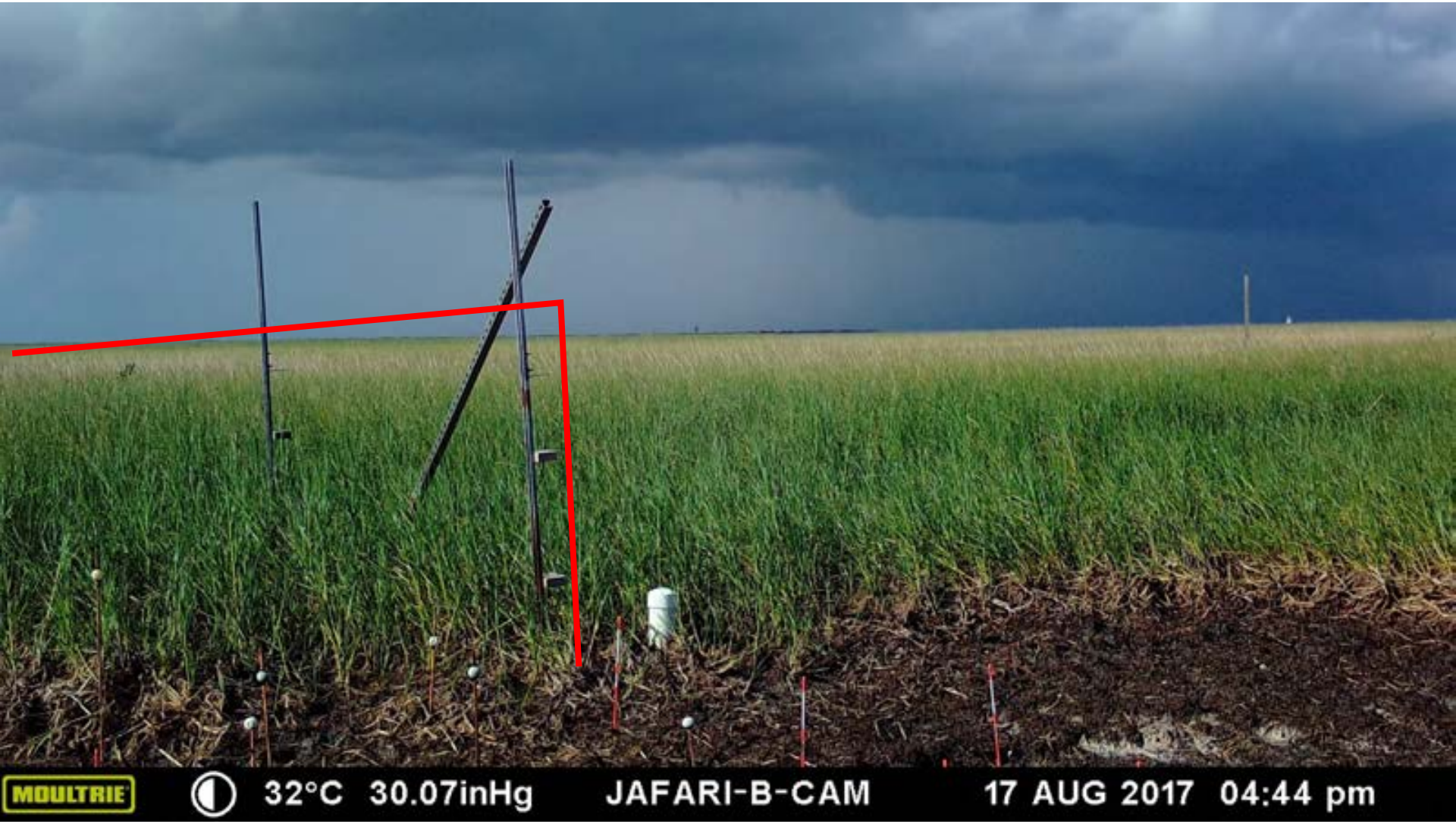

Camera B Time Lapse Photos

Camera B Time Lapse Photos

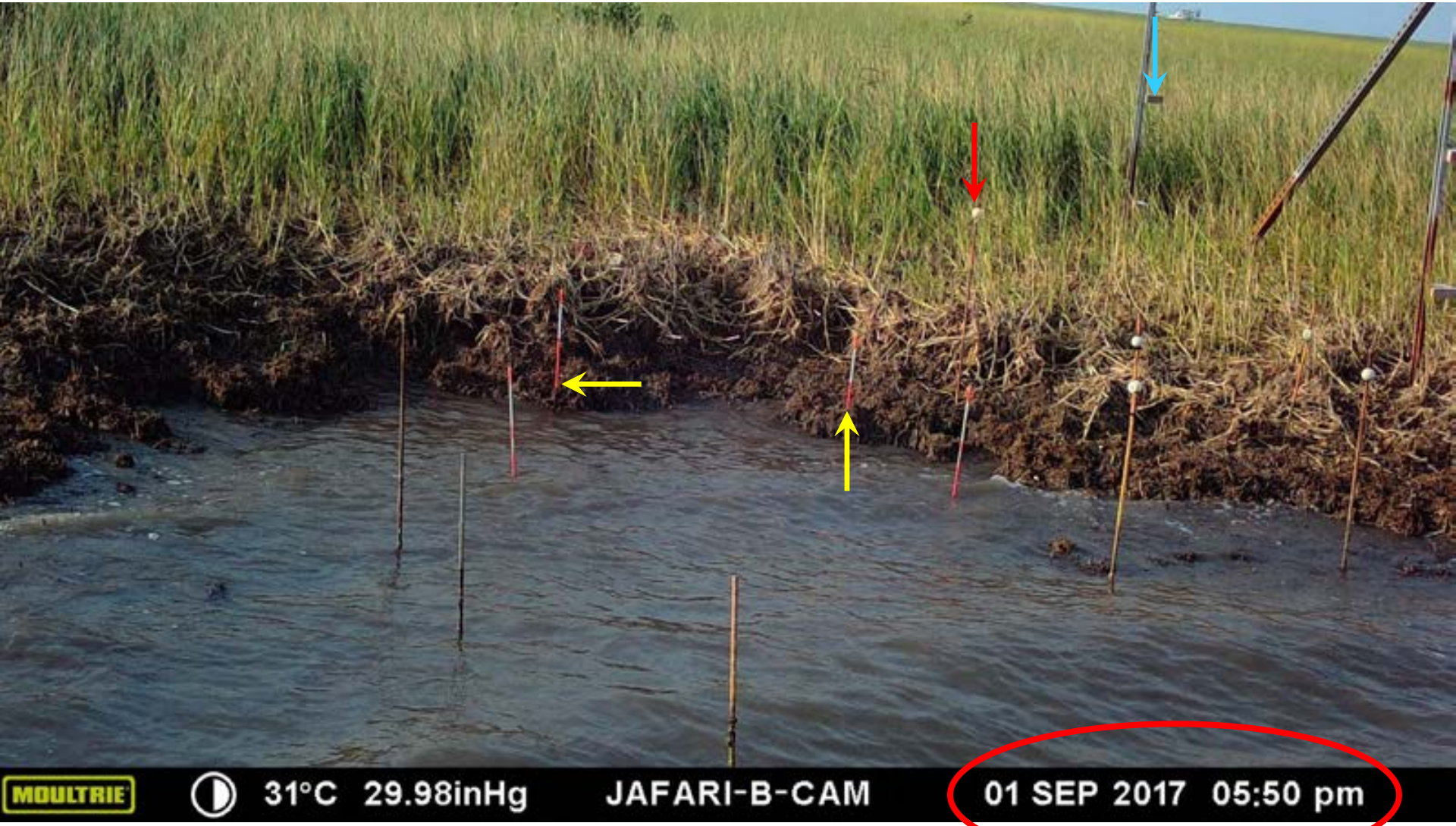

Camera B Time Lapse Photos

Camera B Time Lapse Photos

Camera B Time Lapse Photos

Camera B Time Lapse Photos

Camera B Time Lapse Photos

Camera B Time Lapse Photos

Camera B Time Lapse Photos

Camera B Time Lapse Photos

Camera B Time Lapse Photos

Camera B Time Lapse Photos

Camera B Time Lapse Photos

Camera B Time Lapse Photos

Camera B Time Lapse Photos

Camera B Time Lapse Photos

Camera B Time Lapse Photos

Camera B Time Lapse Photos

Camera B Time Lapse Photos

Camera B Time Lapse Photos

Camera B Time Lapse Photos

Camera B Time Lapse Photos

Camera B Time Lapse Photos

Camera B Time Lapse Photos

Camera B Time Lapse Photos

Camera B Time Lapse Photos

Camera B Time Lapse Photos

Camera B Time Lapse Photos

Camera B Time Lapse Photos

Time-lapse Imagery of Marsh Edge Erosion

Field Installation (August 17, 2017)

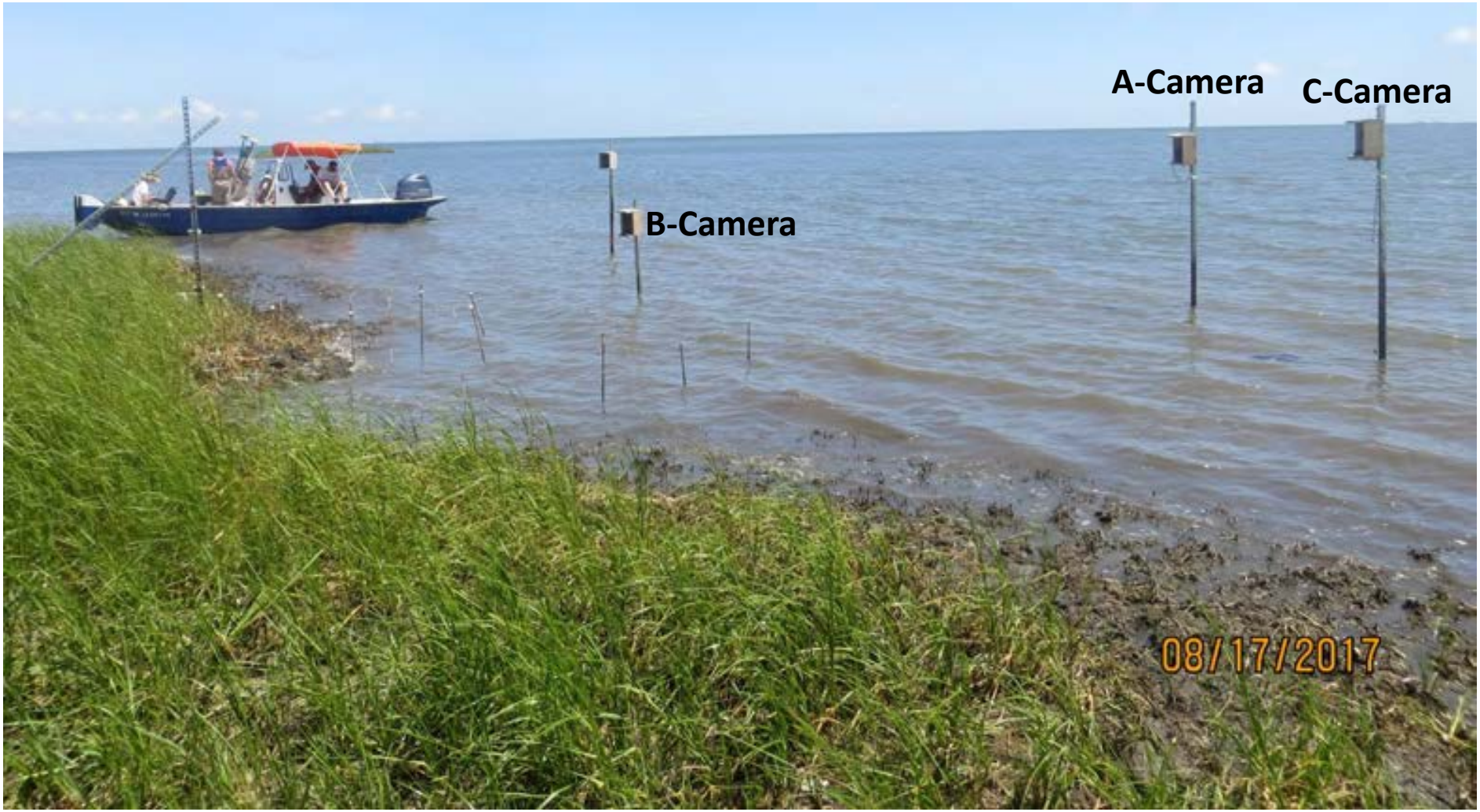

Camera C Time Lapse Photos

Camera C Time Lapse Photos

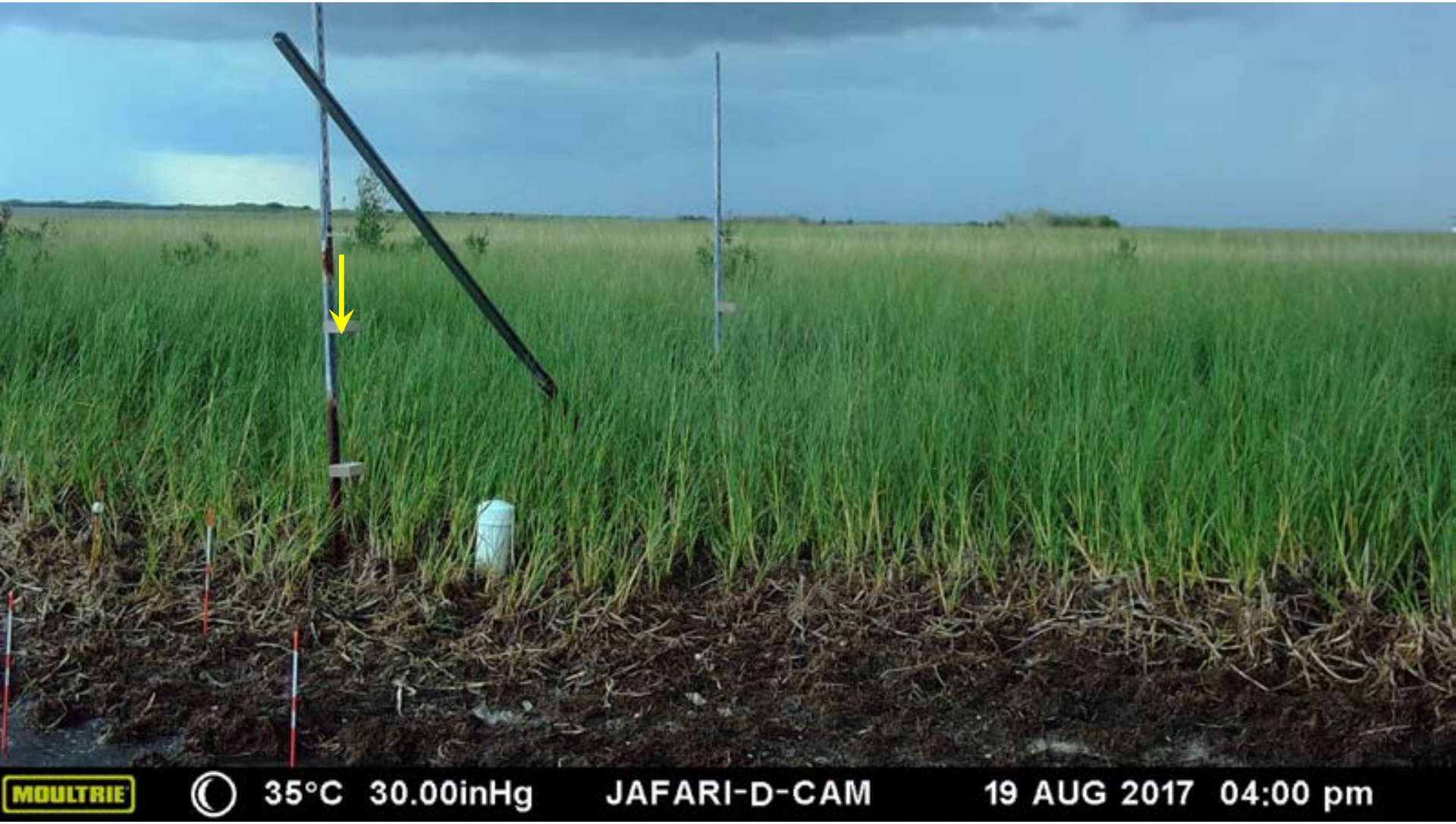

Camera C Time Lapse Photos

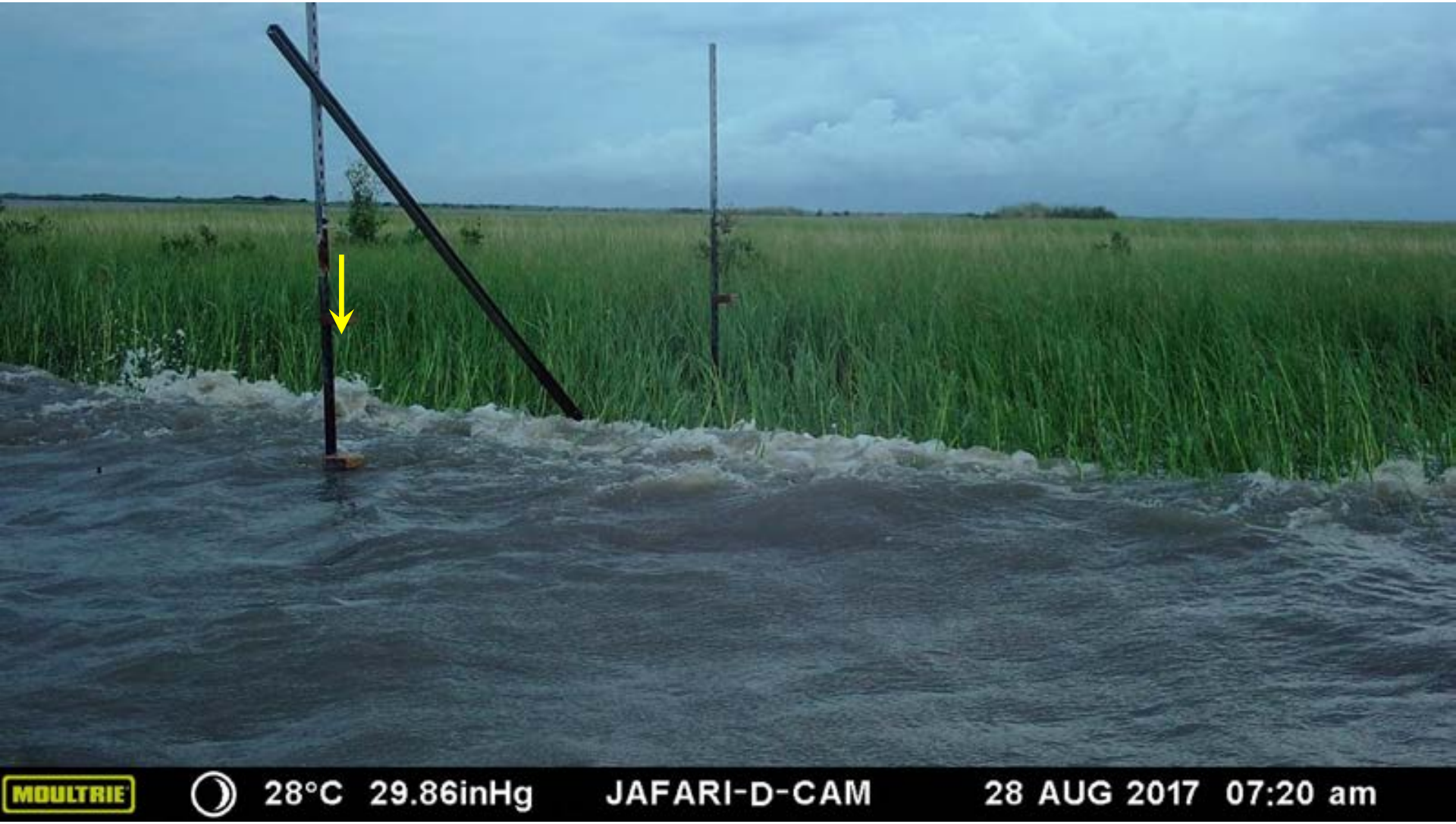

Camera C Time Lapse Photos

Camera C Time Lapse Photos

Camera C Time Lapse Photos

Camera C Time Lapse Photos

Camera C Time Lapse Photos

Camera C Time Lapse Photos

Camera C Time Lapse Photos

Camera C Time Lapse Photos

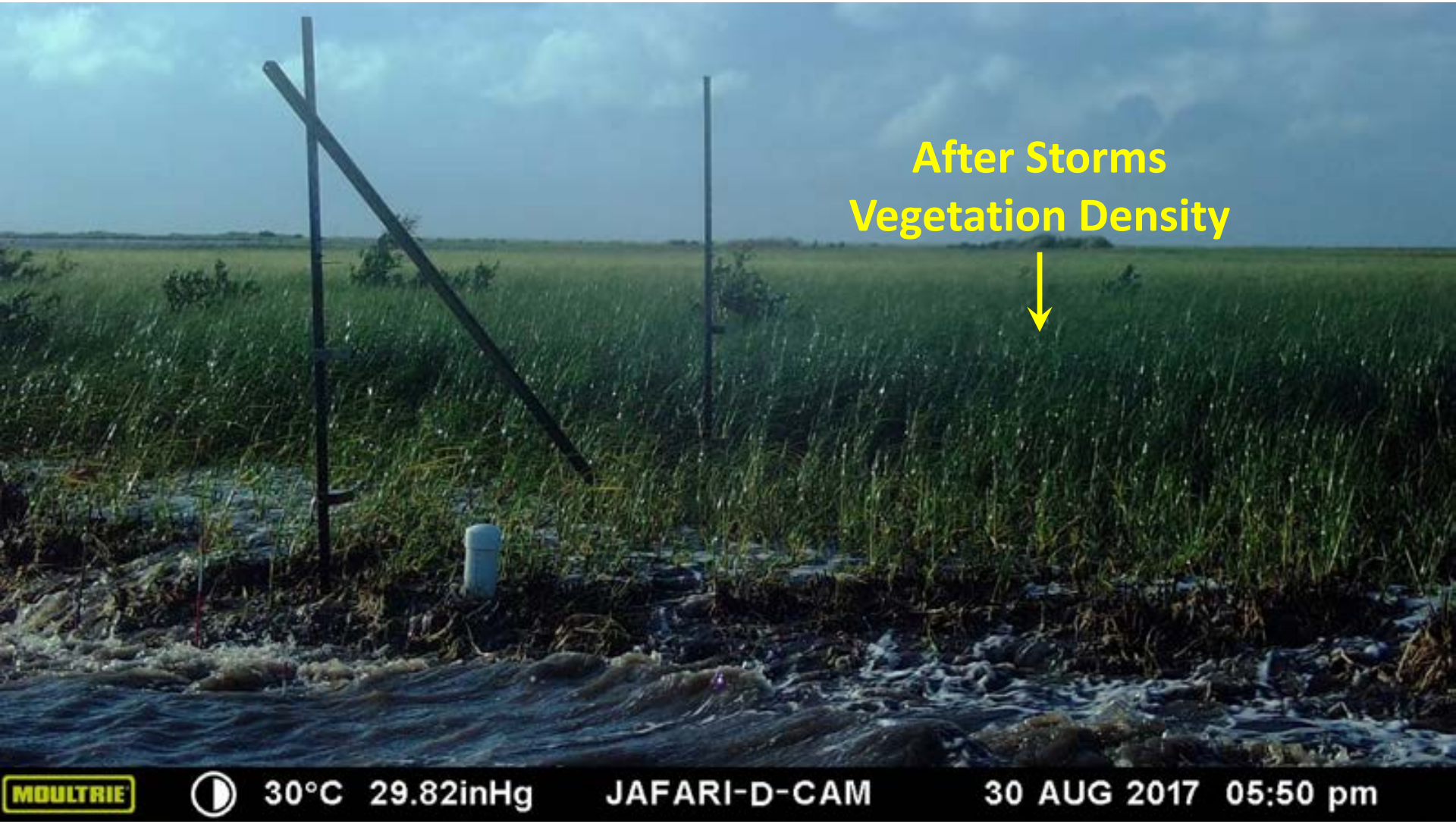

Camera C Time Lapse Photos

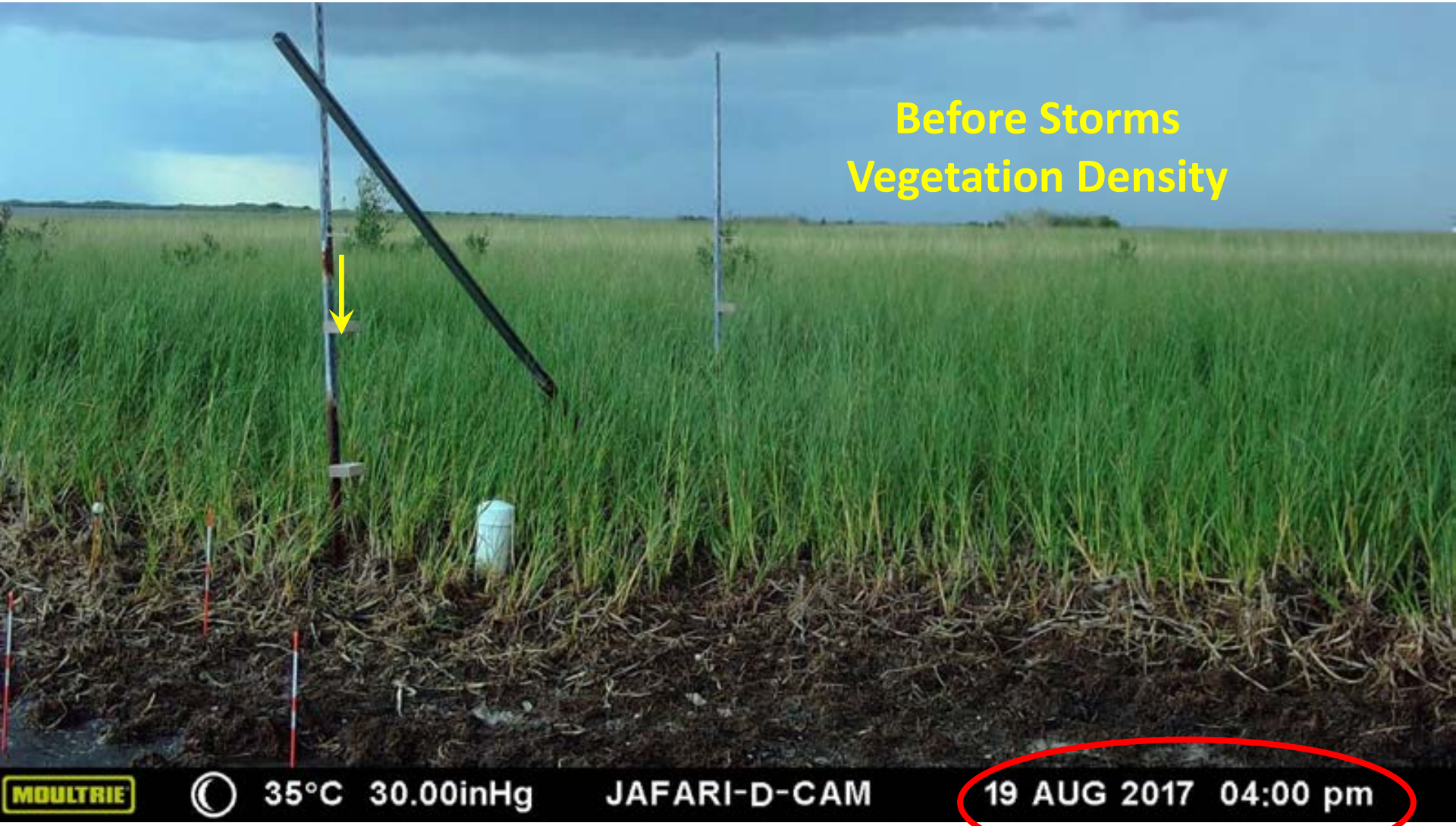

Camera C Time Lapse Photos

Camera C Time Lapse Photos

Camera C Time Lapse Photos

Camera C Time Lapse Photos

Camera C Time Lapse Photos

Camera C Time Lapse Photos

Camera C Time Lapse Photos

Camera C Time Lapse Photos

Camera C Time Lapse Photos

Camera C Time Lapse Photos

Camera C Time Lapse Photos

Camera C Time Lapse Photos

Camera C Time Lapse Photos

Camera C Time Lapse Photos

Camera C Time Lapse Photos

Camera C Time Lapse Photos

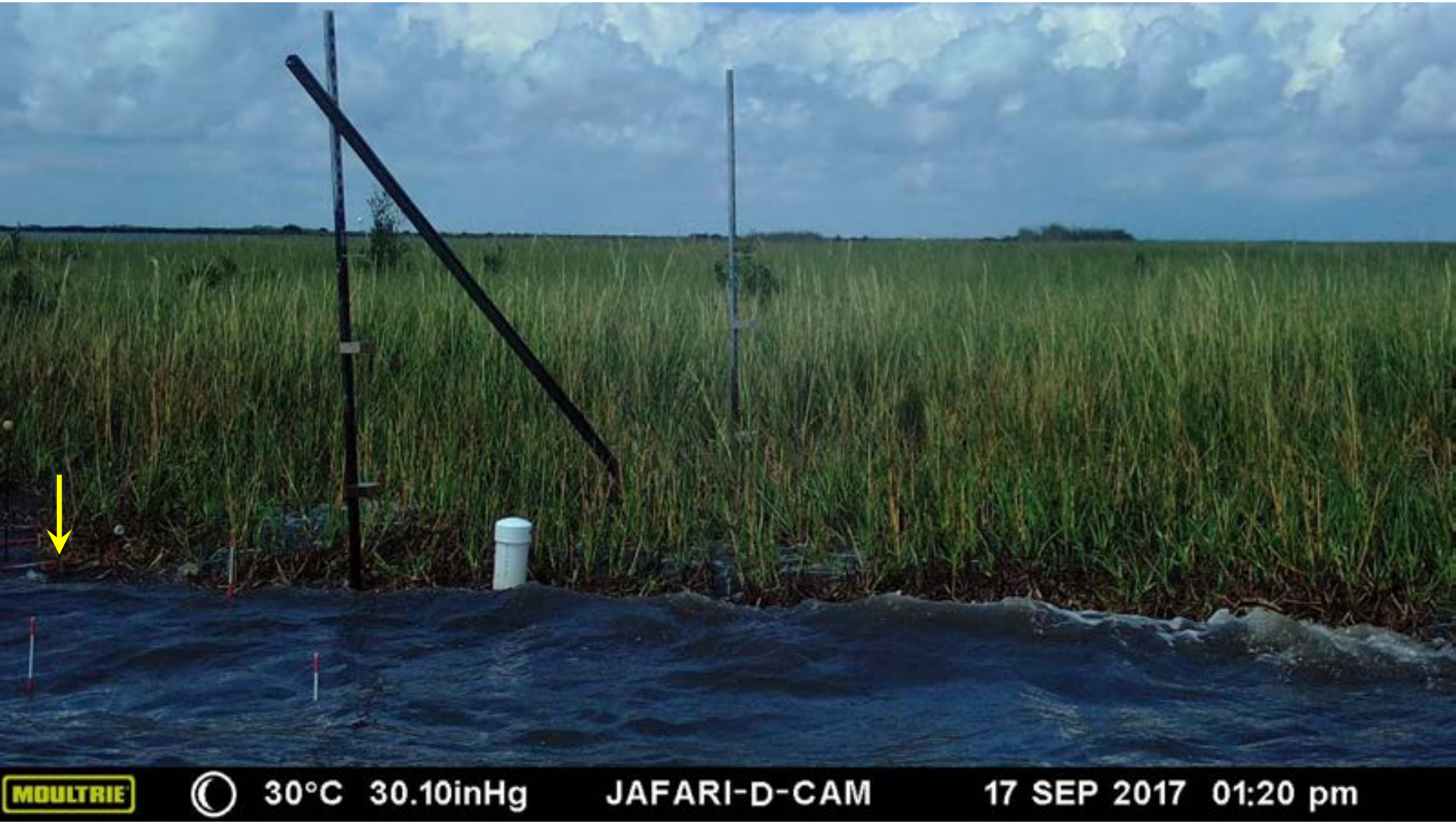

Camera C Time Lapse Photos

Camera C Time Lapse Photos

Camera C Time Lapse Photos

Camera C Time Lapse Photos

Camera C Time Lapse Photos

Camera C Time Lapse Photos

Camera C Time Lapse Photos

Camera C Time Lapse Photos

Camera C Time Lapse Photos

Camera C Time Lapse Photos

Camera C Time Lapse Photos

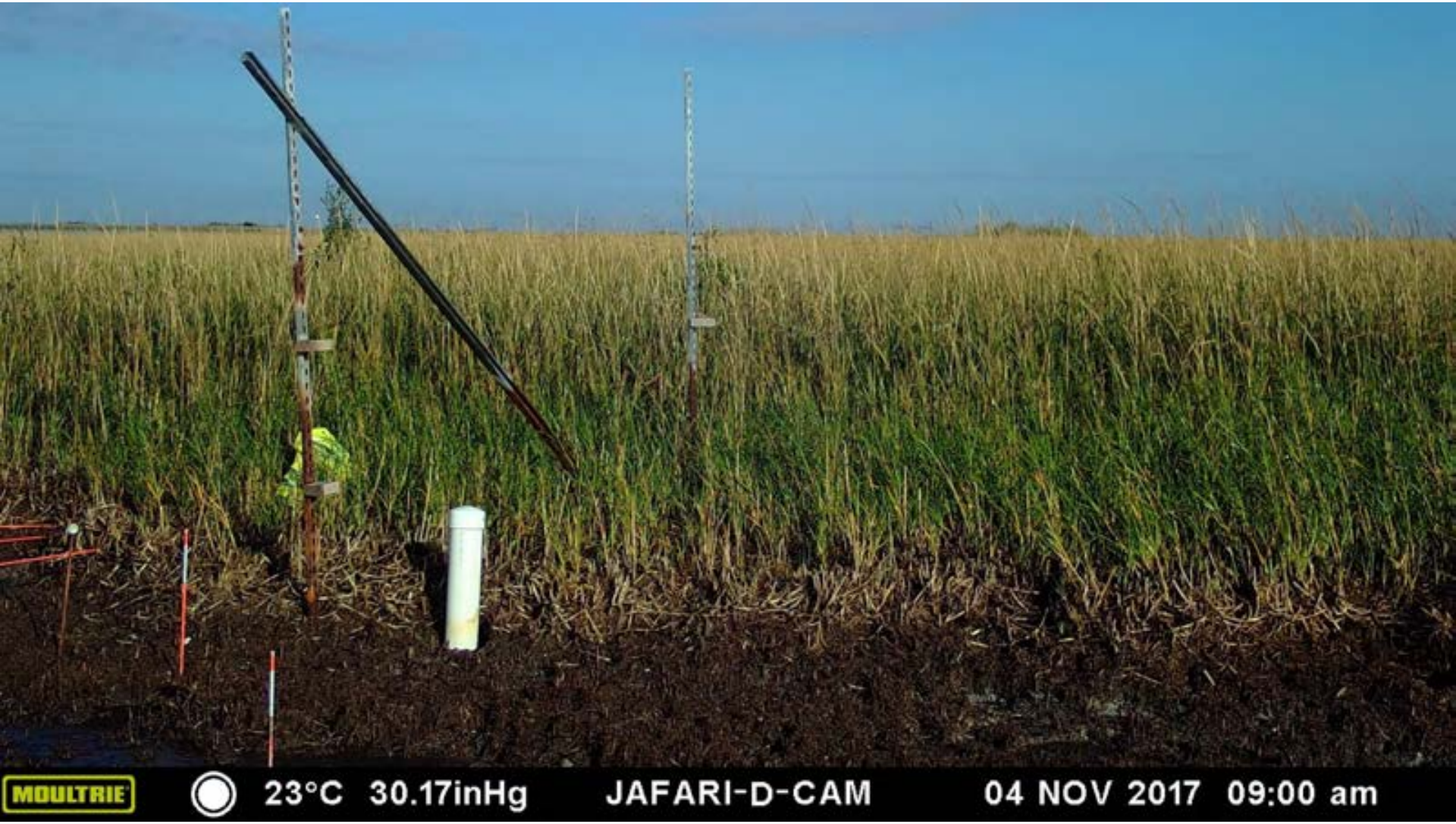

Camera C Time Lapse Photos

Camera C Time Lapse Photos

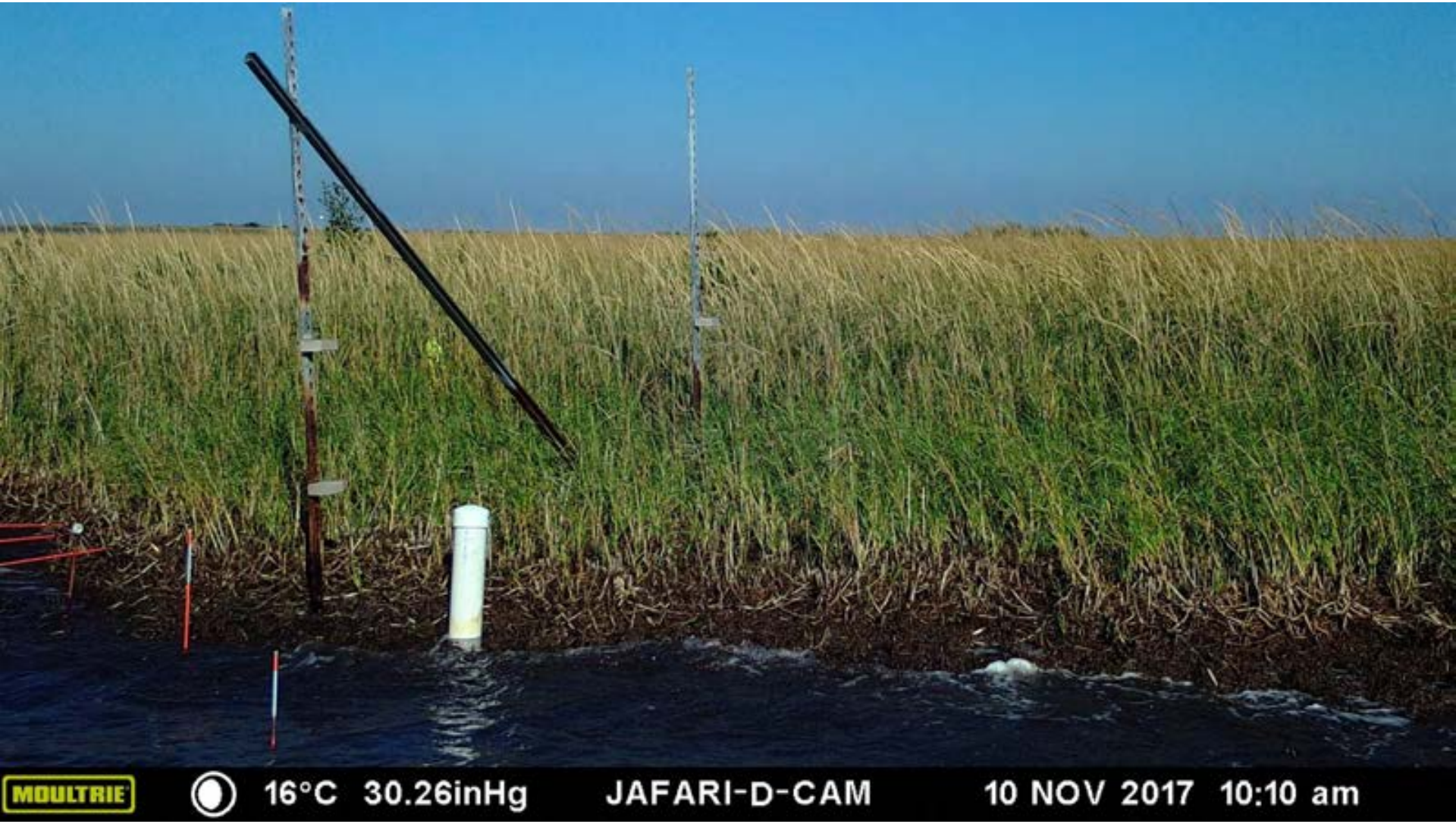

Camera C Time Lapse Photos

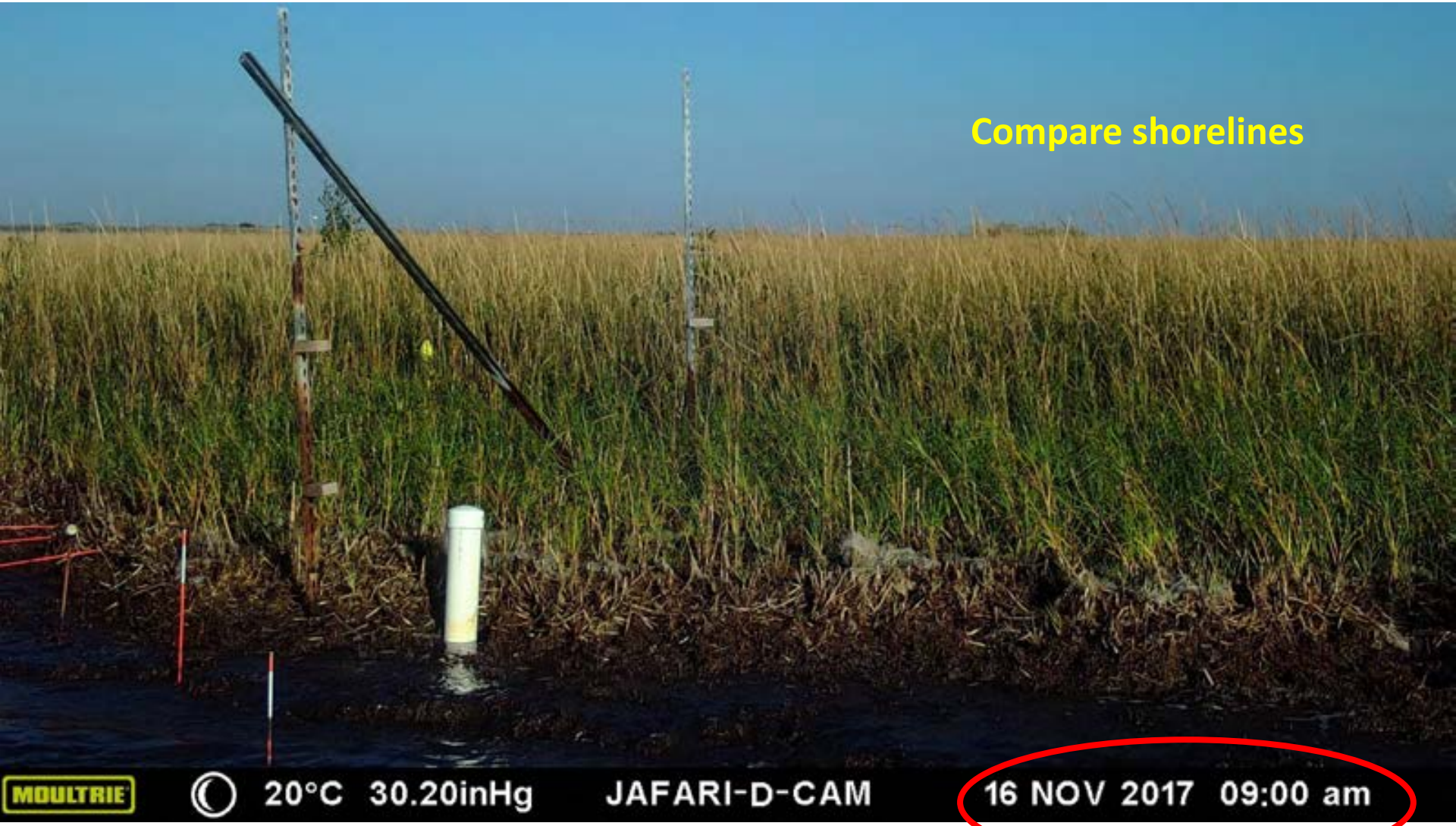
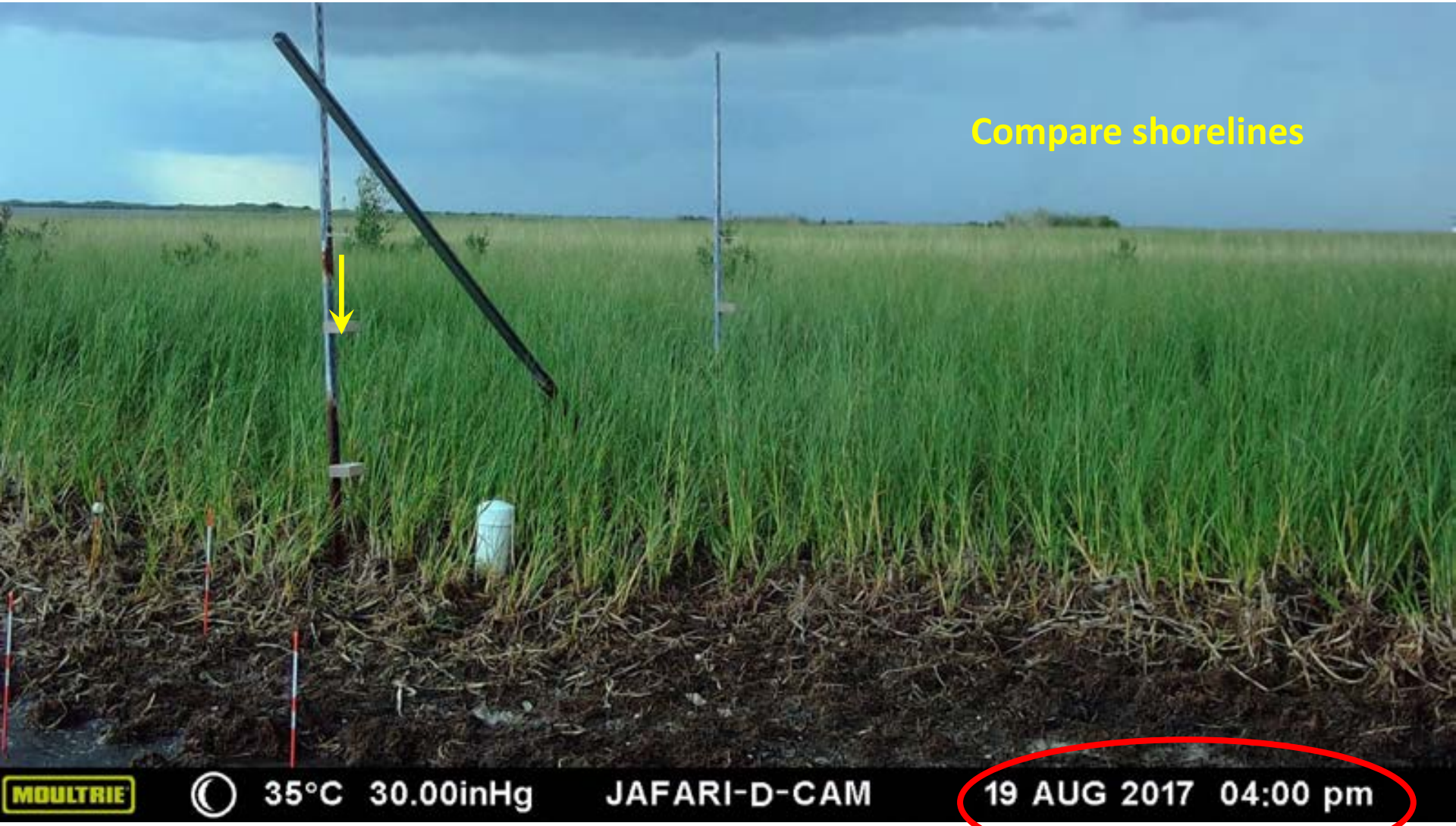
Camera C Time Lapse Photos